Journal of Medicinal Chemistry Article

J. Med. Chem. **2010,** *53,* 573–585 **573**
DOI: 10.1021/jm900838g

Discovery of 4-[(2*S*)-2-{[4-(4-Chlorophenoxy)phenoxy]methyl}-1-pyrrolidinyl]butanoic Acid (DG-051) as a Novel Leukotriene A4 Hydrolase Inhibitor of Leukotriene B4 Biosynthesis†

Vincent Sandanayaka,[‡] Bjorn Mamat,[§] Rama K. Mishra,[‡] Jennifer Winger,[‡] Michael Krohn,[‡] Li-Ming Zhou,[‡] Monica Keyvan,[‡] Livia Enache,[‡] David Sullins,[‡] Emmanuel Onua,[‡] Jun Zhang,[‡] Gudrun Halldorsdottir,[§] Heida Sigthorsdottir,[§] Audur Thorlaksdottir,[§] Gudmundur Sigthorsson,[§] Margret Thorsteinnsdottir,[§] Douglas R. Davies,[∥] Lance J. Stewart,[∥] David E. Zembower,[‡] Thorkell Andresson,[§] Alex S. Kiselyov,[‡] Jasbir Singh,[‡] and Mark E. Gurney*[,‡,§,∥]

[‡]*Medicinal Chemistry, deCODE Chemistry, Inc., 2501 Davey Road, Woodridge, Illinois 60517,* [§]*Drug Discovery, deCODE Genetics, Sturlgata 8, IS-101, Reykjavik, Iceland, and* [∥]*deCODE Biostructures, Inc., 7869 NE Day Road West, Bainbridge Island, Washington 98110*

Received June 9, 2009

Both in-house human genetic and literature data have converged on the identification of leukotriene 4 hydrolase (LTA_4H) as a key target for the treatment of cardiovascular disease. We combined fragment-based crystallography screening with an iterative medicinal chemistry effort to optimize inhibitors of LTA_4H. Ligand efficiency was followed throughout our structure−activity studies. As applied within the context of LTA_4H inhibitor design, the chemistry team was able to design a potent compound **20** (DG-051) (K_d = 26 nM) with high aqueous solubility (> 30 mg/mL) and high oral bioavailability (> 80% across species) that is currently undergoing clinical evaluation for the treatment of myocardial infarction and stroke. The structural biology−chemistry interaction described in this paper provides a sound alternative to conventional screening techniques. This is the first example of a gene-to-clinic paradigm enabled by a fragment-based drug discovery effort.

Introduction

We recently reported the identification of sequence variants in the FLAP[a] and LTA_4H genes that were associated with enhanced capacity for the production of leukotriene B_4 (LTB_4) and increased risk for myocardial infarction (MI) and stroke.[1,2] These conditions feature inflammatory damage to the arterial wall via the formation of atherosclerotic plaque followed by its rupture and consequent thrombosis.[3] Inflammatory cell infiltration, LTB_4 biosynthetic enzymes, and LTB_4 production are increased in atherosclerotic plaque.[4−6]

Literature evidence further suggests that leukotrienes mediate vascular and cellular immune responses in asthma, allergy, and inflammatory diseases.[7] Leukotriene synthesis inhibitors and cysteinyl leukotriene receptor antagonists have shown efficacy in the clinic, resulting in a number of launched therapeutic products (e.g., (*N*-(1-benzo[*b*]thien-2-ylethyl)-*N*-hydroxyurea), zileuton (A-64077),[8] (1-((((1*R*)-1-(3-((*E*)-2-(7-chloro-2-quinolinyl)vinyl)phenyl)-3-(2-(2-hydroxy-2-propanyl)phenyl)propyl)sulfanyl)methyl)cyclopropyl)acetic acid, montelukast,[9] and cyclopentyl(3-(2-methoxy-4-(((2-methylphenyl)sulfonyl)carbamoyl)benzyl)-1-methyl-1*H*-indol-5-yl)-carbamate, zafirlukast (ICI 204,219).[10] LTA_4H is a key enzyme in the leukotriene pathway, which catalyzes the final and rate-determining step in the synthesis of LTB_4.[11] Earlier studies[12] of the potential role of LTA_4H in disease have focused on allergy,[13] dermatitis,[14] and arthritis[15] with a variety of inhibitors[16] reported in the literature (Figure 1).

Several fragment-based drug discovery approaches for screening low molecular weight (< 300 Da) compounds have been reported in the literature, and these include X-ray crystallography, nuclear magnetic resonance (NMR), surface plasmon resonance, differential thermal denaturation, fluorescence polarization, and other techniques.[17−20] In our structure-based approach, we used X-ray crystallography for both identification of hits and their subsequent structure-based evolution into advanced molecules. In our effort to maintain drug-like characteristics of the optimized molecules, in addition to obtaining their bound pose and tracking improvement in enzyme inhibitory activity (IC_{50}) for the intended molecular target, we also followed indices such as BEI (binding efficiency index), SEI (surface efficiency index), and LE (ligand efficiency) that simultaneously track three crucial variables: potency, polar surface area, and molecular weight.[21,22] On the basis of the analysis of over 120 marketed drugs, a range of optimal values (SEI = 18 ± 8.7, BEI = 28 ± 7.9, and LE ∼ 0.4), for these indices have been provided as a guide.[23]

Results and Discussion

Initially, crystals of LTA_4H were grown (Supporting Information for details) and soaked with our fragment library,

†Protein Data Bank coordinates have been deposited under the following accession codes: compound **2** bound to LTA_4H, 3FHE; compound **5** bound to LTA_4H, 3FH8; compound **8** bound to LTA_4H, 3FTZ; compound **9** bound to LTA_4H, 3FUL; compound **14** bound to LTA_4H, 3FH5; compound **20** bound to LTA_4H, 3FH7.

*To whom correspondence should be addressed. Phone: 1-630-635-0937. Fax: 1-630-783-4646. E-mail: mark.gurney@decode.is. Address: Mark E. Gurney, Ph.D., Sr. VP, Drug Discovery and Development, 2501 Davey Road, Woodridge, IL 60517.

[a] Abbreviations: APA, aminopeptidase A; APP1, aminopeptidase P1; APN, aminopeptidase N; AUC, area-under the curve; BEI, binding efficiency index; BSA, bovine serum albumin; CVD, cardiovascular diseases; FLAP, 5-lipoxygenase activating protein inhibitor; FOL, fragments of life; LTA_4H, human leukotriene A4 hydrolase; HWB, human whole blood; SEI, surface efficiency index; LE, ligand efficiency; LRAP, leukocyte-derived arginine aminopeptidase; PILS, puromycin-insensitive leucyl-specific aminopeptidase; PK, pharmacokinetic.

Published on Web 12/01/2009

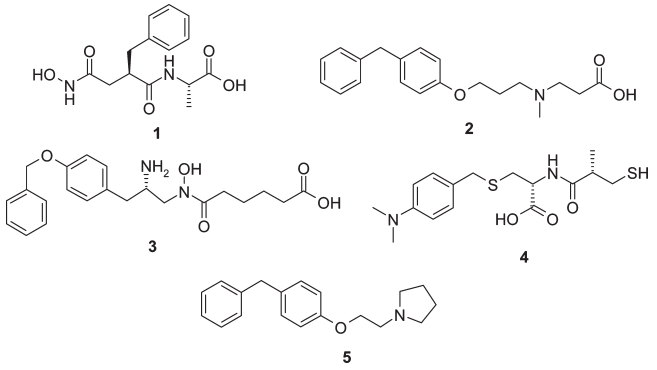

Figure 1. LTA_4H inhibitors reported in the literature.[13]

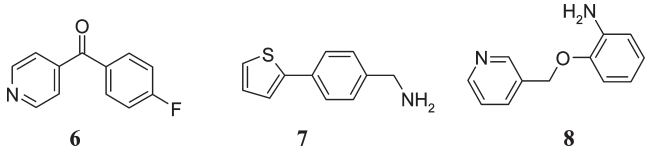

Figure 2. Structures of bound biaryl/hHeteroaryl FOL fragments.

termed "fragments of life" (FOL).[24] This customized set of ~1300 lead-like small molecules[20] is composed of natural metabolites, their derivatives, and heterocyclic derivatives that mimic protein-turn motifs (e.g., α-, β-, and γ-turns). These compounds have high solubility and chemical features allowing rapid synthetic elaboration. The FOL library, clustered into 6−8 diverse fragments per pool, was soaked with LTA_4H crystals and hits were reconfirmed by X-ray crystallography with a single fragment. This expedited approach provided several diverse biaryl/heteroaryl fragments bound to LTA_4H as chemical leads for further elaboration. The structures of three fragments are shown in Figure 2; their binding modes at the hydrophobic L-shaped active site pocket are shown in Figure 3. For each of the identified fragments, we observed both hydrophobic packing as well as specific hydrogen bond interactions with either crystallographic water (ex., ligand **6**, N−O (water) = 3.2 Å), active site residues (ex. ligand **8** with CO of Pro374), or water mediated interactions with active site residues (ex., ligand **7** with Gln136). The observed inhibition of LTA_4H hydrolysis (IC_{50} = 5.38 mM, 98 μM, and > 2 mM and for fragments **6**, **7**, and **8**, respectively) by these fragments prompted their further elaboration. The enzyme assay used recombinant human LTA_4H with LTA_4 as the substrate to determine IC_{50} values (see Experimental Section, Biological Assays). In several instances, we found an acetate anion recruited from the crystallization media to bind to the catalytic zinc in the active site of LTA_4H. An acetate bound to zinc was observed in the absence (not shown) or presence of a bound fragment in the hydrophobic pocket (Figure 3). This mapping of two distinct binding sites by the biaryl fragments and an acetate anion provided our initial hypothesis for the overall trajectory of an LTA_4H inhibitor to be pursued by structure-based design. The SEI/BEI for fragments **6** and **7** were 7.6/11.3 and 7.4/21.1, respectively. A combination of factors including active site fit, synthetic feasibility, and ligand efficiency prompted us to select **6** for further optimization.

In the next series of experiments, we continued with our iterative chemistry−structural biology studies. Our focus was to (i) capture additional interactions in the hydrophilic pocket by chemical elaboration of the biaryl fragments and (ii) evaluate linking of the two identified fragments, biaryl and acetate. Considering both literature evidence[25] and our structural insight, we endowed fragment **6** with an *N*-pyrrolidine ethanol moiety (Figure 4) to result in analogue **9**. In our hands, the binding mode of **9** to LTA_4H (Supporting Information Figure SF1b) was consistent with the observed pose for **6**. However, analogue **9** contained two potentially disruptive interactions with the enzyme. These were between the carbonyls of **9** and Trp311 and between the pyridinyl nitrogen of **9** and the oxygen of water WAT-33, which were in close proximity (ligand CO−CO (Trp311) = 3.0 Å and N−O (WAT-33) = 3.12 Å). Thus, we observed only limited improvement in LTA_4H inhibition for **9** vs **6** (IC_{50} = 199 and 5380 μM, respectively). These limitations were addressed in analogue **5**, which did not feature any of these repulsive interactions (Supporting Information Figure SF1c) and consequently showed potent enzyme inhibition (IC_{50} = 180 nM). The binding mode of compound **2** (Supporting Information Figure SF1d) provided further insight into chemical design. X-ray crystallographic data showed good complementarity between the biaryl moiety and the hydrophobic surface of the active site channel. We also observed an ionic interaction of the carboxylate group with the Zn ion (Zn^{2+}−COO^- distance = 1.49 Å). This −COO−Zn contact is contrary to previously published data based on extended X-ray absorption fine structure (EXAFS) spectroscopy of LTA_4H, which concluded that there was a lack of interaction of carboxylate containing inhibitors with the zinc atom of the enzyme.[26] As anticipated, molecule **5** also featured sound ligand efficiency (0.44), although it displayed very high SEI value (54.1).

Combining the structural evidence accumulated thus far, we explored a series of functional groups to tether the identified biaryl fragments to the carboxylate. A number of linkers were considered and evaluated, with a goal for the optimized linker to capture additional interactions with LTA_4H active site residues. Representative examples of these linkers are shown in Supporting Information Figure SF2: (a) the pyridine analogue **10** is based on potentials for capturing π−π, π-to-edge or π−cation interactions with Tyr267 and (b) replacement of the ether oxygen of **5** with tertiary nitrogen, yielding piperazine analogues **11** and **12**, which were designed to fill the available volume and to mediate interaction with Gln134/Gln136. Structures of analogues **10**−**12** are shown in Figure 4. Analogue **10** showed relatively weak inhibitory activity (IC_{50} = 8.7 μM), while derivatives **11** and **12** displayed better inhibitory potency (IC_{50} = 1.4 and 0.340 μM, respectively). The bound poses of the pyridine analogue **10** and the iodo-analogue **12** are shown in Supporting Information, parts a and b of Figure SF3, respectively.

Despite a good fit into the binding pocket, moieties featuring a tertiary amine group in compounds **2** and **5** showed no direct interaction with Gln134 and Gln136 (Supporting Information Figure SF1c,d). In a subsequent chemical modification, we replaced the aminoethylether chain of **5** with either (*S*) or (*R*) prolinol to result in molecules **13** and **14** (Figure 5a). Both enantiomeric derivatives, (*S*)-isomer **13** and (*R*)-isomer **14**, provided improved activity compared to analogue **5** (IC_{50} = 244 and 87 nM, respectively). Moreover, the pyrrolidine nitrogen of **13** and **14** is positioned to exert strong interactions with Gln134 (2.76 Å) and Gln136 (2.83 Å) (Figure 5b,c), as evidenced from the structural studies. The side chain of Gln134 underwent a ligand induced conformational change from its native position in the enzyme[27] to accommodate the interactions with **14**. This side chain

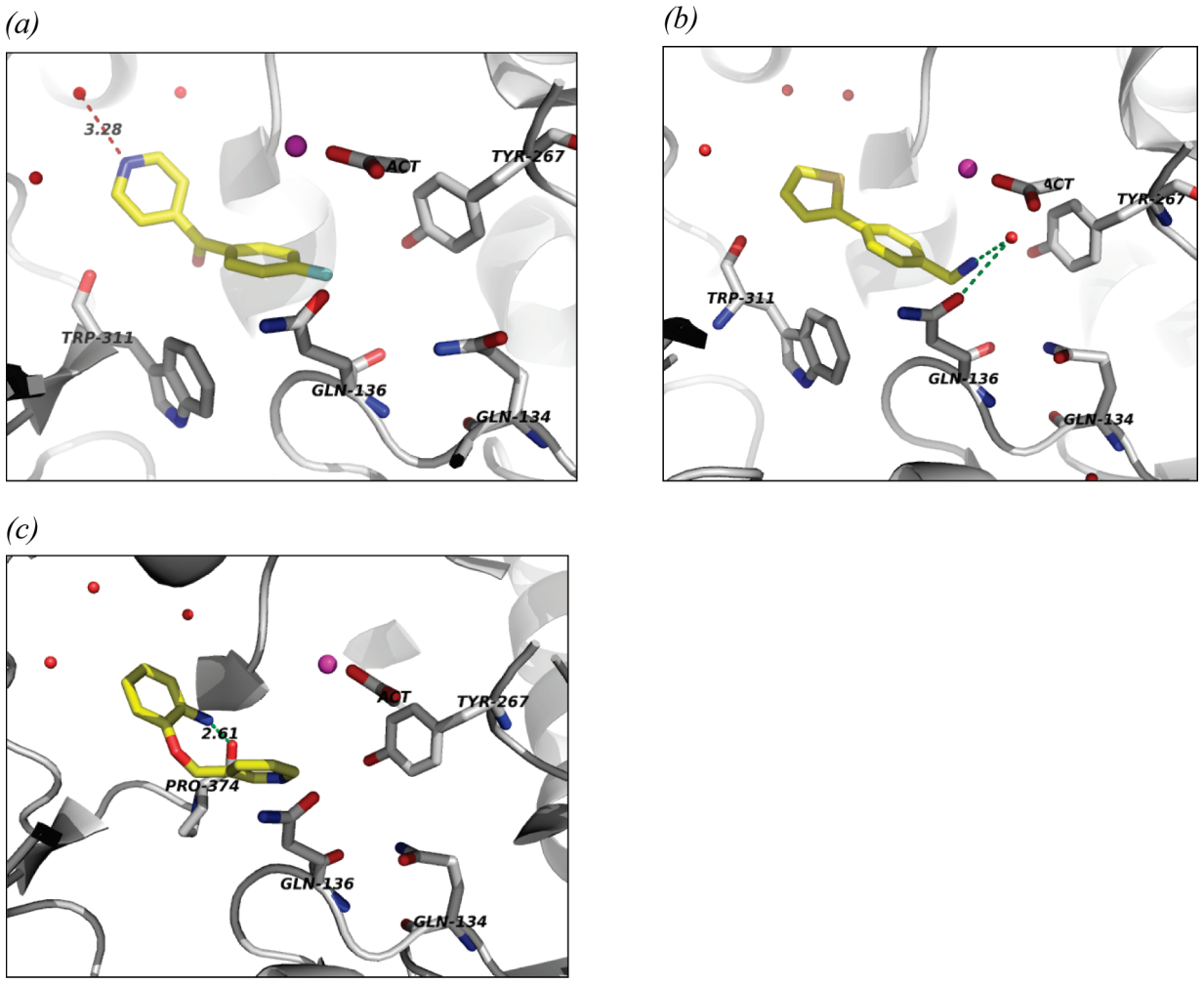

Figure 3. Bound pose of biaryl fragments at the hydrophobic pocket and acetate bound to catalytic zinc. (a) Fragment **6** with N−O (water) = 3.2 Å and Zn−$OCOCH_3$ = 1.98 Å, resolution 1.8 Å; (b) fragment **7** and acetate with Zn−$OCOCH_3$ = 1.98A, resolution 2.0 Å; (c) fragment **7** and acetate with Zn−$OCOCH_3$ = 2.19 Å, resolution 2.05 Å. In each figure, acetate (labeled as ACT) is bound to active site zinc. The catalytic Zn ion is shown in magenta and water molecules are shown as red spheres.

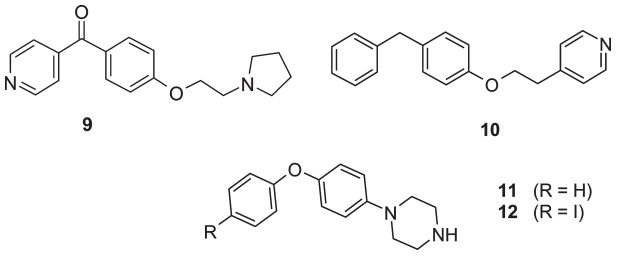

Figure 4. Structures of analogues **9**−**12**.

rotamer led to the formation of a new hydrogen bond between the amide nitrogen of Gln134 and the peptidyl oxygens of Gln136 (2.82 Å) and Gln134 (intraresidue hydrogen bond, 3.04 Å) (Figure 5b). The X-ray cocrystal structure of the corresponding (*S*)-enantiomer **13** revealed a weaker interaction with Gln136 (3.35 Å), whereas Gln134 retained its original orientation. In support of the observed 3-fold difference in potency, cocrystal structures of **13** lacked the hydrogen bond network observed for its enantiomer **14** (Figure 5c). For both ligands, the methyleneoxy chain between the biphenyl group and the pyrrolidine ring afforded optimal positioning of the ligand within the LTA_4H binding pocket (Figure 5b,c). Of the evaluated linkers, the prolinol-derived ligand impacted

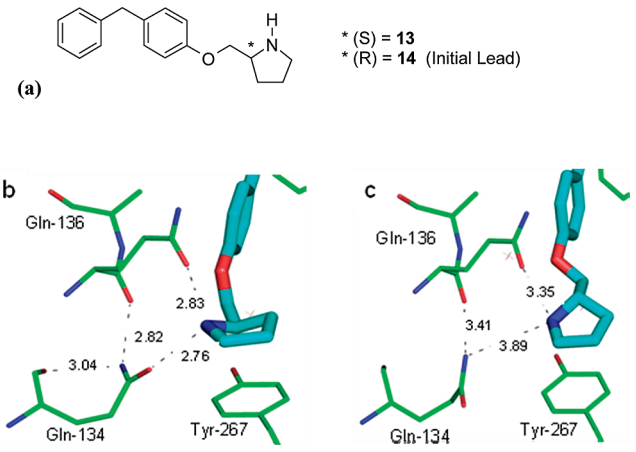

Figure 5. (a) Shows the chemical structures for the (*S*) and (*R*) prolinol-derived analogues **13** and **14**, respectively, and (b) and (c) shows bound orientations of (*S*) and (*R*) prolinol-derived analogues **13** and **14**, respectively. (b) Hydrogen bond network involving Gln134 and Gln136 in the complex with **14**. (c) Identical view for the corresponding (*S*) enantiomer, **13**. Note: in the bound poses of these two enantiomers, Gln134 has different orientation, with orientation of G1n134 with **14** being identical to that in the apoenzyme (not shown).

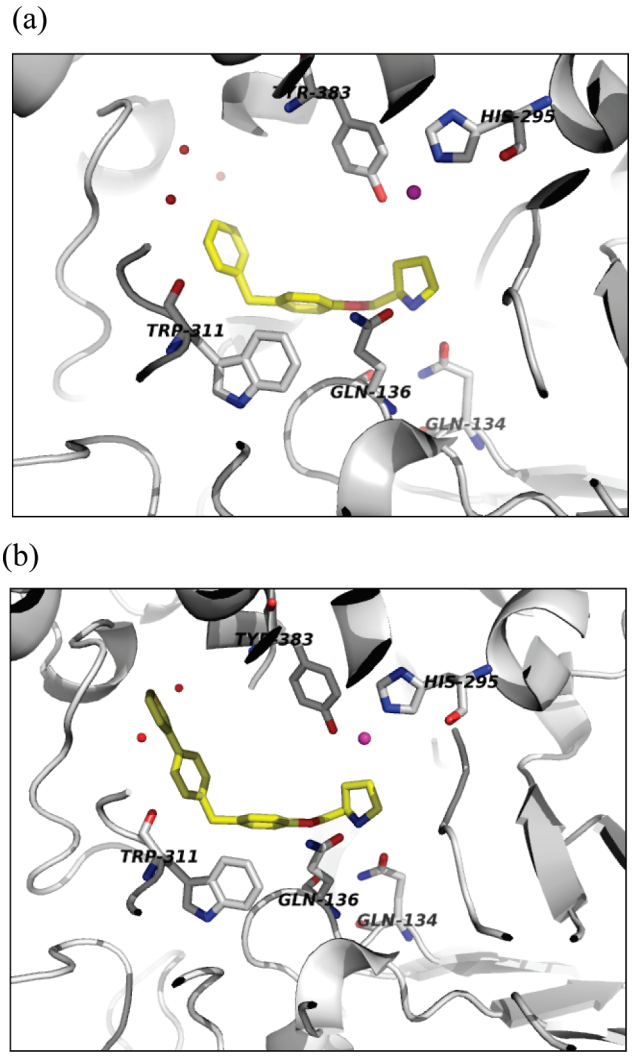

Figure 6. Displacement of "structural" water molecule with *para*-3′-thienyl group of ligand **15**. (a) X-ray cocrystal structure of LTA_4H in complex with **14** at 1.63 Å resolution showing three crystallographic waters in the hydrophobic pocket and (b) X-ray cocrystal structure of **15** at 1.69 Å resolution showing only two crystallographic water molecules in the hydrophobic pocket. The thiophene has displaced the center water molecule present in (a). The catalytic Zn ion is shown in magenta and water molecules are shown as red spheres.

the Gln134 side chain movement the most, securing it as a tether of choice for subsequent ligand elaboration.

We attempted further optimization by varying the nature of the biaryl group. Considering the hydrophobic nature of the pocket occupied by this pharmacophore, we incorporated lipophilic substituents onto the terminal phenyl ring. Substitution at the para-position was projected to displace one or more of the three conserved water molecules deep within the active site pocket (Figure 6a), thus potentially improving affinity of the molecule toward LTA_4H and blocking the anticipated cytochrome P450 (CYP) mediated metabolism at this site. We found that relatively large groups including thiophenes and thiazoles did in fact displace the central water molecule (WAT-762) as in the cocrystal structure of **14** (Figure 6b), and these modifications provided potent LTA_4H inhibitors. Compound **15** showed a 21-fold improvement in enzyme inhibitory activity ($IC_{50} = 4$ nM) vs the unsubstituted analogue **14** ($IC_{50} = 87$ nM). Unfortunately, these derivatives

Table 1. Biological and Pharmacological Data for Selected Compounds

compd	**14**	**17**	**20**
IC_{50} (nM) (enzyme)	87	30	47
K_d (nM)	ND	ND	25
IC_{50} (nM) (HWB)[†]	449	533	37
pK_a[a]	10.41	10.39	4.02, 8.35 ($pI = 6.18$)[b]
microsome stability[c]	10.5	86.6	95.2
PK parameters[d]			
species	rat	mouse	rat	dog	monkey
dose (mg/kg)	10	10	10	10	10
$t_{1/2}$ (h)[e]	0.67	3.59	2.57	4.02	5.54
C_{max} (μM)[f]	1.46 (iv)	1.02	4.8	19.3	18.9
AUC (h·ng/mL)	471 (iv)	2362	12968	56045	52410
%F[g]	ND	85	87	252	186
V_d (mL/kg) (iv)[h]	6121	6324	2351	1564	2073
Cl (mL/min/kg) (iv)[I]	71.0	61.0	11.0	7.6	6.0

[a] pK_a values are calculated using ACD laboratories software for **14** and **17**, and experimental values are reported for compound **20** ($pK_{a1} = 4.02$, $pK_{a2} = 8.35$). [b] Isoelectric constant. [c] Microsome stability indicates parent remaining after 30 min incubation in human liver microsomes. [d] Unless otherwise indicated, pharmacokinetic (PK) values are for oral administration (po). [e] The plasma elimination half-life, $t_{1/2}$, was determined by linear regression of the terminal phase of the logarithm plasma concentration−time curve. [f] The maximum plasma concentration (C_{max}) is the observed peak plasma concentration after an oral dose. [g] Oral bioavailability (F%) was determined using AUC (area under the plasma concentration−time curve from time zero to infinity normalized for dose) in po, (except when indicated for iv) [h] Volume of distribution. [I] Predicted clearance. ND = not determined.

were found to be cytotoxic and relatively nonspecific in a broad panel screen (Cerep) for off-target activity.[28] Replacement of the heterocycle with a *p*-chlorine substituent to yield **16** addressed the issue of cellular toxicity. As shown by structural studies, the *para*-Cl group did not displace the bound water molecules. Values for the three ligand efficiency indices were: LE = 0.21 for compound **6** and 0.24 for compound **10** vs LE = 0.49 for compound **14**, and SEI and BEI = 7.6 and 11.3 for compound **6** vs 33.1 and 26.4 for compound **14**, respectively. Thus, the structure-guided elaboration of fragment **6** to compound **14** was on track for simultaneously enhancing key ligand parameters (Supporting Information Table ST1 and Figure SF4).

As reported above, we found that **14** inhibited LTA_4H with an IC_{50} of 87 nM. In a physiologically relevant secondary assay, human whole blood (HWB) was used to assess inhibition (IC_{50}) of LTB_4 production after stimulation with Ca^{2+} ionophore (see Experimental Section, Biological Assays). In this assay, **14** showed an IC_{50} of 449 nM, a 5-fold decrease compared to the in vitro data. The cocrystal structure of **14** bound to the enzyme is shown in Figure 6b.

In an attempt to further optimize compound **14**, we replaced the methylene bridge with an ether moiety providing compound **17** with a 2-fold increase in enzyme inhibitory potency ($IC_{50} = 49$ nM) and HWB assay ($IC_{50} = 284$ nM). The X-ray analysis confirmed an essentially identical binding mode for **17**. This modification also afforded improvement in key PK parameters, such as half-life and systemic exposure (for **14** $t_{1/2} = 0.67$ h; $AUC_{0-Inf} = 471$ h·ng/mL and for **17**: $t_{1/2} = 3.6$ h; $AUC_{Inf} = 2362$ h·ng/mL), presumably due to eliminating metabolism at the methylene site (Table 1).

Focusing on the second binding element revealed by fragment screening, the acetate ion bound to the catalytic zinc (Figure 3), we optimized the carboxylic acid pharmacophore by introducing carbon chains of variable length between the

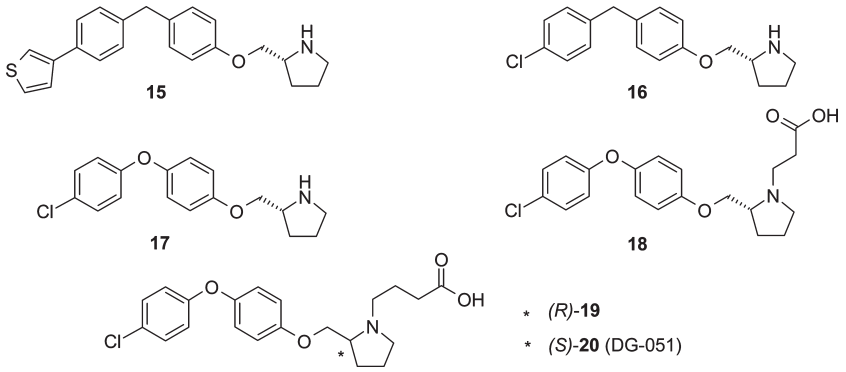

Figure 7. Advanced intermediate and the clinical candidate compound.

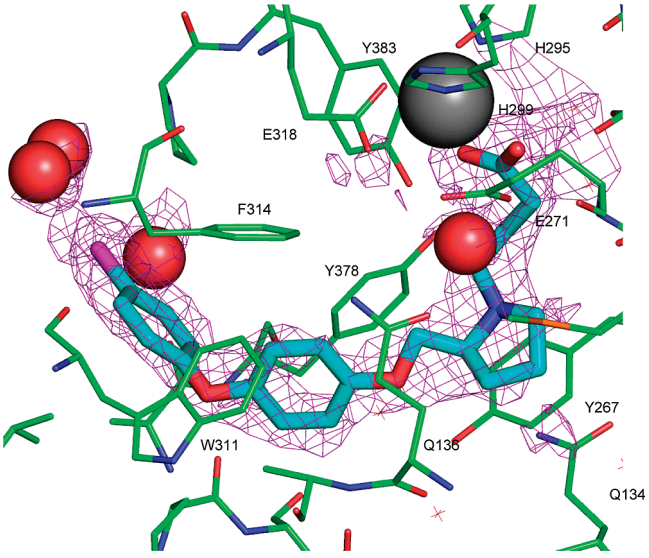

Figure 8. X-ray cocrystal structure of **20** in complex with LTA_4H showing the displacement of two water molecules located near Zn by the carboxylic acid group. The $F_o - F_c$ electron density map is contoured at 2σ.

pyrrolidine nitrogen and the carboxylate. Both two- and three-carbon chains containing carboxylic acid derivatives (**18** and **19**, Figure 7) showed comparable activities in the enzyme assay and were potent in the HWB assay with IC_{50} values of 23 and 33 nM, respectively. A two-carbon linker previously was reported in compound **2** to undergo metabolic *N*-oxidation followed by Cope reaction to furnish acrylic acid and *N*-hydroxyl amine leading to toxicity in vivo.[29] On the basis of our concern that **18** may undergo similar metabolic conversion, the butyric acid derivative **19** featuring a three-carbon linker was selected for further evaluation.

Given the relatively high cost of D-proline, the corresponding (*S*)-enantiomer derived from L-proline was prepared for comparison (**19** and **20**, respectively). These molecules were equipotent in the HWB assay (IC_{50} = 33 and 37 nM, respectively). Therefore, the synthetically more feasible (*S*)-enantiomer **20** was identified as the lead compound for further evaluation. The X-ray crystal structure of **20** bound to LTA_4H showed that the carboxylate displaced two of the three water molecules near Zn^{2+} by chelating to the metal. One oxygen of the carboxylate group was a direct ligand of Zn^{2+} adopting a slightly distorted tetrahedral coordination geometry with His295, His299, and Glu318, while the second oxygen interacts with Glu296 and the remaining water molecule (WAT-545 in the **20** structure) of the solvent cluster (Figure 8). Compound **20** was a potent inhibitor in the enzyme assay with an IC_{50} = 47 nM. Although the molecule gained binding affinity through interaction with Zn^{2+}, in contrast to **14** it did not participate in hydrogen-bond interactions with Gln136 or Gln134, although the tertiary nitrogen (of **20**) appears to show water mediated interaction with Glu271. Inhibitor **20** provided over 4-log improvement in activity compared with the biaryl compound **6** that was identified through crystallographic screening of our in-house fragment library.

Although useful for screening and rank ordering of compounds for inhibitory potency, the in vitro enzyme assay was formatted as an end-point assay. It required relatively high concentrations of both the enzyme and bovine serum albumin (BSA) in the reaction mixture (see Experimental Section, In Vitro Enzyme Assay). Therefore, we used isothermal microcalorimetry to determine the equilibrium dissociation constant, K_d, of **20** binding to LTA_4H. The measured value of 25 nM compared favorably against both enzymatic and whole blood assay data, suggesting lack of significant plasma binding and high cellular permeability for the molecule.

The introduction of the carboxylic acid group into **20** allowed for the optimization of other compound properties. Specifically, aqueous solubility at the isoelectric point (pH ~ 6.18) was high (> 30 mg/mL), streamlining formulation and oral administration protocols for **20**. The molecule showed good absorption and low clearance across all species tested with very high oral bioavailability (Table 1). The half-life in dog and monkey predicted a similar value in human, sufficient to allow once daily dosing. Furthermore, for compound **20**, we were able to lower the volume of distribution (V_d ~2000 mL/kg) compared to early compounds (**14** and **17**), resulting in higher plasma concentration. Considering our target indication, it is beneficial to have more drug in the systemic circulation than in the tissues, as blood cells and the vessel wall are the main target compartments in cardiovascular diseases. Very high values of C_{max} and AUC based on dose across all species indicated the potential for good in vivo potency. It is worth noting that compound **20** both displayed excellent PK profile across various species as well as good physicochemical properties. This molecule also featured excellent ligand efficiency [(LE = 0.38), BEI (18.8), and SEI (12.4)], values similar to several successful marketed drugs.[20] Thus, crystallography driven medicinal chemistry optimization provided compound **20** with enhanced potency against its molecular target (LTA_4H).

Off-Target Activity Profiling. The activity and selectivity of **20** was assessed in a variety of in vitro assays. LTA_4H is a

Scheme 1[a]

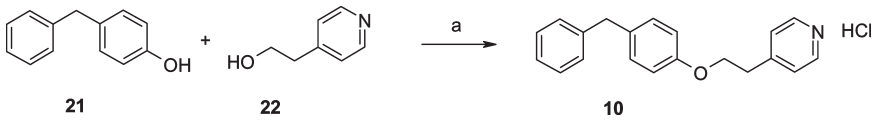

21 **22** **10**

[a] (a) PPh_3, DIAD, THF, 70 °C, 27%.

Scheme 2[a]

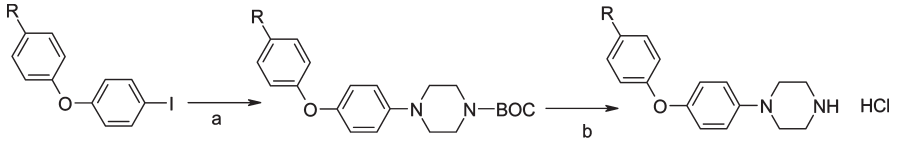

23 (R=H) **24** (R=I) **25** (R=H) **26** (R=I) **11** (R = H) **12** (R = I)

[a] (a) $(nBu)_3P$, $Pd(dba)_2$, Na-OtBu, toluene, reflux, BOC-piperazine, 25−75%; (b) 4 N HCl/*p*-dioxane, 95−98%.

Scheme 3

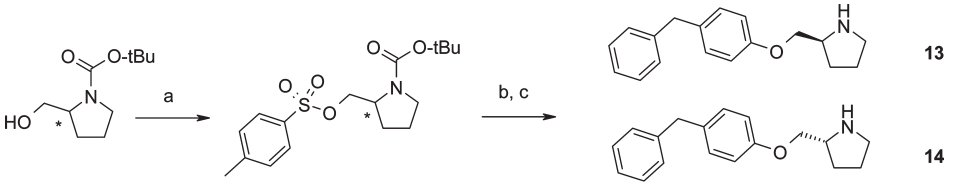

27 * = (S)-enantiomer **28** * = (R)-enantiomer **29** * = (S)-enantiomer **30** * = (R)-enantiomer

(a) Py/TsCl, 91−99%; (b) NaH, DMF, (**21**); (c) 4 N HCl/*p*-dioxane, 73%.

dual function enzyme with both hydrolase and aminopeptidase activities. Substrates for the two reactions occupy overlapping regions of the active site and both reactions are catalyzed by the zinc ion. Compound **20** was a potent inhibitor of LTA_4H aminopeptidase activity against L-alanine *p*-nitroanilide (IC_{50} = 72 nM). In assessing potential liability related to off-target activities, compound **20** was screened in vitro against a panel of more than 50 targets including aminopeptidases (APN, LRAP, PILS, APP1, and APA), ion channels, human cardiac ERG channel, G-protein coupled receptors, and nuclear receptors known to mediate side effects in the clinical setting. No significant inhibition (defined as > 50% at 10 μM) was observed for any of the targets tested. We also assessed the potential liability of **20** for drug−drug interaction through inhibition of cytochrome P450 isozymes. The ability of **20** to interfere with in vitro metabolic activity of major human CYPs was determined using heterologously expressed human CYP 1A2, 2C9, 2C19, 2D6, and 3A4.[30] No inhibition greater than 50% was observed with any of the above CYPs against their substrates using **20** at 10 μM concentration. These data, along with low overall metabolism of **20** and the low predicted plasma exposures to reach an IC_{90} for LTA_4H inhibition suggested that clinically relevant inhibition of major human CYPs is unlikely.

Compound **20** was profiled for activity in a number of in vivo models of inflammation using reduction in LTB_4 production as a biomarker.[2,3] These studies will be reported in subsequent publications elsewhere. Compound **20** currently is in human phase II clinical trials for the prevention of myocardial infarction and stroke.

Chemistry. Compound **9** was prepared as reported previously.[21] Compound **10** was prepared by Mitsunobu reaction[31] of 4-benzylphenol and 4-pyridyl ethanol (Scheme 1). Synthesis of the piperazine derivatives **11** and **12** was accomplished by reaction of mono-BOC protected piperazine under Buchwald conditions,[32] (using Bu_3P, $Pd(dba)_2$, and NaOtBu as a base in refluxing toluene) from 1-iodo-4-phenoxy-benzene (**23**) and 1-iodo-4-(4-iodophenoxy) benzene (**24**), respectively, to provide **25** and **26**. Subsequent deprotection of the N-BOC group under acidic conditions provided the desired compounds **11** and **12** (Scheme 2).

Synthesis of prolinol derived analogues **13** and **14** was accomplished by the nucleophilic displacement of the tosyl group of **29** and **30**, respectively, with the phenolate derived from 4-benzylphenol **21** (Scheme 3), followed by removal of the BOC protecting group. Tosylates **29** and **30** were prepared following the literature procedure[33] from (*S*)- and (*R*)-BOC-prolinol, respectively (Scheme 3).

The Friedel−Crafts acylation of anisole with benzoyl chlorides **31a**/**31b** followed by reduction of the ketones (**32a**/**32b**) with triethylsilane/trifluoroacetic acid provided phenyl methyl ethers **33a**/**33b**. Removal of methyl ethers **33a**/**33b** with boron tribromide in CH_2Cl_2 provided the phenols **34a**/**34b**, respectively. Suzuki−Miyaura coupling[34] of **34b** with thiophene-3-boronic acid using Pd/C provided phenol **35**. The sodium phenolate of **35**, generated in situ with NaH in DMF, was subsequently reacted with tosylate **30**. Deprotection of the *N*-BOC intermediate **36** under acidic conditions provided the compound **15**. Similarly, phenol **34a** was elaborated to provide the BOC protected amine **37**. Deprotection of the BOC with HCl in *p*-dioxane, followed by

Scheme 4[a]

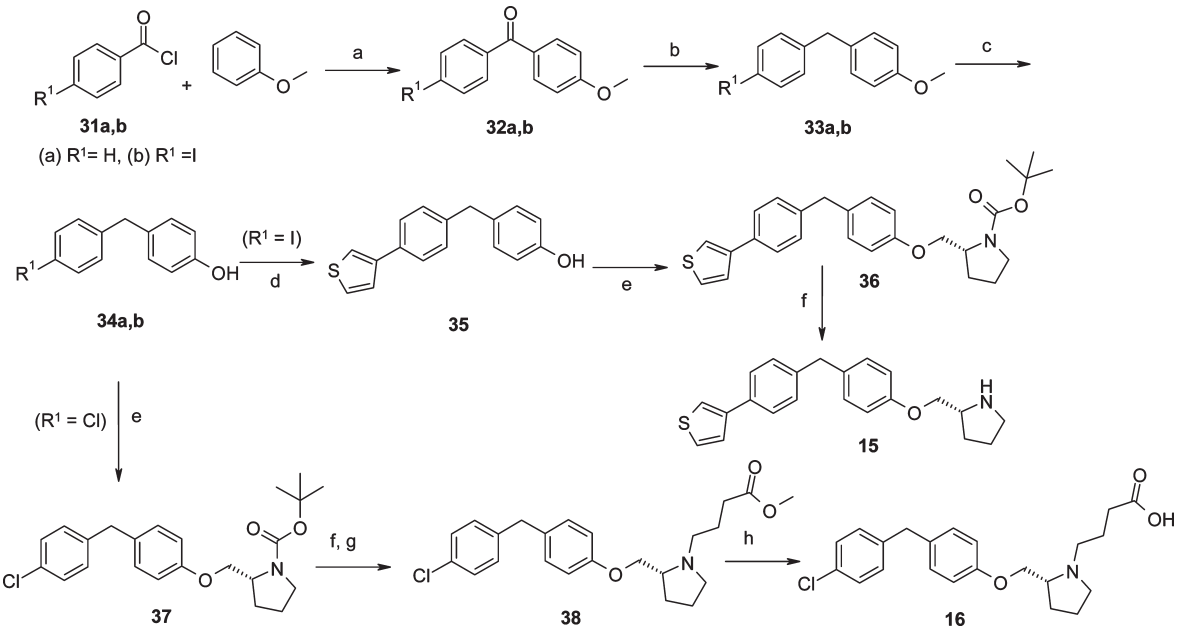

[a] (a) $AlCl_3$, nitrobenzene, 90%; (b) Et_3SiH, TFA, 99%; (c) BBr_3, CH_2Cl_2; (d) 3-thiophene-boronic acid, K_2CO_3, Pd/C, iPrOH/H_2O, 99%; (e) NaH, DMF, (**30**); (f) 4 N HCl/*p*-dioxane, 53% (from **35** to **15**); (g) K_2CO_3, DMF, $Br(CH_2)_3CO_2CH_3$, rt, 35%; (h) NaOH, MeOH, 87%.

Scheme 5[a]

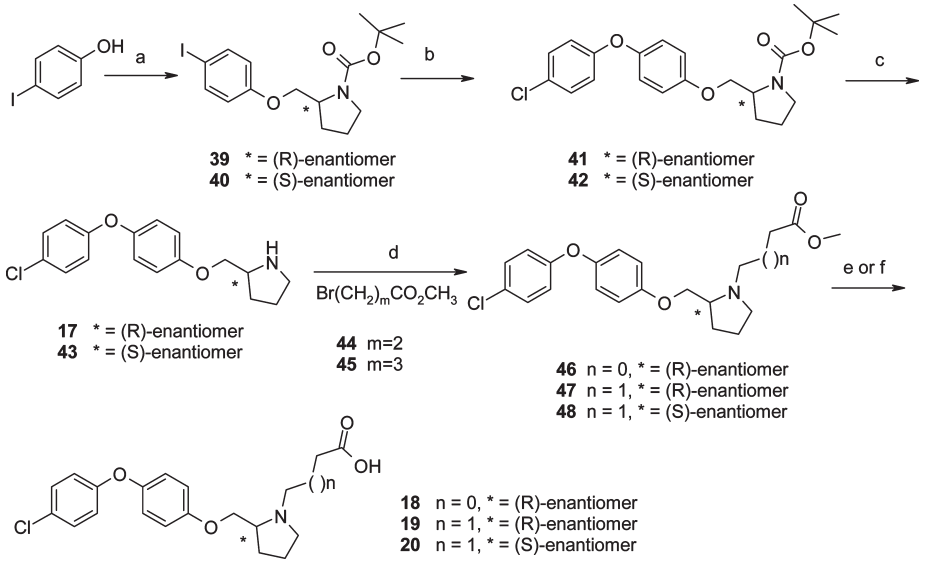

[a] (a) KO-tBu, DMF, (**29**) or (**30**), 92%; (b) *N*,*N*-dimethylglycine, Cs_2CO_3, Cu(I), 4-chlorophenol, 56%; (c) 4 N HCl, *p*-dioxane, 83%; (d) K_2CO_3, DMF, (e) aq NaOH, MeOH, 36%; (f) HCl/Et_2O, 93%; (g) (**46**),1:1 conc HCl/*p*-dioxane, 60 °C, 4 h, 68%.

alkylation of the secondary amine with methyl-4-bromobutyrate and subsequent base hydrolysis of the ester (**38**), provided the analogue **16** (Scheme 4).

The general synthesis of the diphenyl ether derivatives **17**−**20** is shown in Scheme 5. Reaction of 4-iodophenol with BOC-tosylates **29** or **30**, using Cu(I) mediated Ullmann coupling[35] of the iodo-phenyl intermediate **39**/**40** with 4-chlorophenol, provided the corresponding diphenyl ether derivatives **41**/**42**. Deprotection of the *N*-BOC derivatives under acidic conditions provided the amine derivatives **17** ((*R*)-enantiomer) and **43** ((*S*)-enantiomer) as hydrochloride salts. Alkylation of the secondary amine (**17** or **43**) with a 4-bromobuterate (**45**) or with 3-bromopropionate under basic conditions provided the corresponding esters (**46**−**48**). The hydrolysis of the esters under basic conditions followed by acidification or under acid hydrolysis conditions provided the desired analogues **19**−**20**.

Conclusion

In summary, the development of **20** illustrates a number of trends in modern drug discovery. These include (a) the use of human population genetic studies to identify new therapeutic targets for major common diseases, (b) the utility of a fragment-based screening for the identification of novel chemotypes empowering optimization studies, and (c) iterative structural biology−medicinal chemistry process leading to

accelerated lead optimization. As a result of the structure-assisted SAR and simultaneous optimization of pharmacokinetics, pharmacodynamics, selectivity, and solubility along with the minimized potential for toxicity, we have identified compound **20** as the clinical candidate. Specifically, our genetic studies linked LTA_4H genes that were associated with increased risk for myocardial infarction (MI) and stroke.[1,2] To the best of our knowledge, this is the first example of a gene-to-clinic paradigm enabled by the iterative use of fragment-based drug discovery and structure-guided medicinal chemistry, providing a candidate optimized for ligand parameters and imparting desirable drug characteristics. DG-051 recently entered human phase II clinical trials in CVD.

Experimental Section

Chemistry. All reagents, starting materials, and anhydrous solvents were obtained from commercial sources and used without further purification unless otherwise noted. Concentration refers to evaporation under vacuum using a Büchi rotatory evaporator. NMR spectra were recorded at 400 or 500 MHz (Varian Instruments) in the solvent indicated, and TMS was used an internal reference. ACDLabs NMR software was used to process FIDs to generate spectral parameters (ppm/Hz). Coupling constants (J) are given in Hz. Mass spectra were obtained using either APCI or electrospray ionization (PE-SCIEX single-quad or Agilent mixed-mode units). Elemental analyses were carried out by Galbraith Laboratories, Inc. (Knoxville, TN) or Midwest Microlab, LLC (Indianapolis, IN). Compounds were purified by flash chromatography using silica gel (MP EcoChrom, 32−63D, 60 Å). Typically, 1:10 to 1:20 ratio of the crude product to silica gel was used. Purity of all final products was determined by analytical HPLC and/or by LC-MS to be ≥95%. HPLC purity of compounds were measured with a reversed-phase HPLC (Phemomenex Prodigy C_{18} column, 4.6 mm × 150 mm, 5 μm, typically at 254 nm, unless indicated) with one of the following two conditions. HPLC-1: compounds were eluted using a gradient of 90/10 to 10/90 A/B over 40 min at a flow rate of 1.0 mL/min, where solvent A was aqueous 0.05% TFA and solvent B was CH_3CN (0.05% TFA). HPLC-2: compounds were eluted using a gradient of 95/5 to 5/95 A/B over 40 min at a flow rate of 1.0 mL/min, where solvent A was aqueous 0.05% TFA and solvent B was CH_3CN (0.05% TFA). For HPLC data, (final products), peak area percent and retention time (t_R in minutes) are provided.

4-[2-(4-Benzylphenoxy)ethyl]pyridine (10). The 4-pyridine ethanol (123 mg, 1.0 mmol) was dissolved in THF (3 mL) and solutions of 4-benzylphenol (240 mg, 1.3 mmol) in THF (1 mL) and Ph_3P (315 mg, 1.2 mmol) in THF (1 mL) were added. The reaction was cooled to 0 °C, and a solution of diisopropyldiazodicarboxylate (242 mg, 1.2 mmol) in THF (1 mL) was added, followed by stirring at rt for 4 h. The reaction was heated to 70 °C and maintained for 16 h. The solvent was removed in vacuo, and the resulting material was purified by silica gel flash chromatography (20−50% EtOAc/hexanes, gradient) and stirred with 2 M HCl in Et_2O (excess) at rt to give the compound **10** as the hydrochloride salt (0.89 g, 27%). MS m/z: 290 (M + H). ^{1}H NMR (400 MHz, DMSO-d_6) δ: 8.80 (d, J = 6.8 Hz, 2H), 7.96 (d, J = 6.8 Hz, 2H), 7.26 (m, 2H), 7.17 (m, 3H), 7.12 (d, J = 8.8 Hz, 2H), 6.84 (d, J = 8.8 Hz, 2H), 4.30 (t, J = 6 Hz, 2H), 3.86 (s, 2H), 3.31 (t, J = 6.3 Hz, 2H). HPLC-1: 99.7%, t_R = 19.5 min.

1-(4-Phenoxyphenyl)piperazine Hydrochloride (11). A solution of 4N HCl in dioxane (30 mL) and **10b** (3.0 g, 8.46 mmol) were stirred at rt for 1 h. EtOAc (30 mL) was added and solid was collected by filtration and washed with EtOAc (2 × 10 mL) and the solid was dried under vacuo to provide the title compound **11** (2.71 g, 98.2%) as a white solid. MS m/z: 255 (M + H). ^{1}H NMR (400 MHz, DMSO-d_6) δ: 9.11 (br s, 1 H) 7.65 (d, J = 8.9 Hz, 2 H) 6.95−7.07 (m, 4 H) 6.75 (d, J = 8.9 Hz, 2 H) 3.30−3.36 (m, 4 H) 3.22 (br s, 4 H).

1-[4-(4-Iodophenoxy)phenyl]piperazine Hydrochloride (12). A solution of 4N HCl in dioxane (15 mL) and **12b** (1.1 g, 2.3 mmol) were stirred at rt for 1 h. EtOAc (30 mL) and hexanes (30 mL) were added and solid was collected by filtration and washed with EtOAc (2 × 15 mL) and the solid was dried under vacuo to provide the title compound **12** (1.11 g, 95%) as an off-white solid. MS m/z: 381 (M + H). LCMS: 98%. ^{1}H NMR (400 MHz, DMSO-d_6) δ: 9.29 (br. s., 1 H) 7.27−7.41 (m, 2 H) 7.01 −7.11 (m, 3 H) 6.89−6.99 (m, 4 H) 3.30−3.36 (m, 4 H) 3.18−3.25 (m, 4 H).

(2*S*)-2-[(4-Benzylphenoxy)methyl]pyrrolidine (13). To a solution of 4-benzylphenol, **21** (0.10 g, 0.56 mmol) in anhydrous DMF (1 mL) at 0 °C was added a 60% dispersion of NaH in mineral oil (0.02 g, 0.75 mmol) portionwise over 5 min. The resulting slurry was stirred at 0 °C for 10 min before a solution of (*S*)-tosylate **29** (0.20 g, 0.56 mmol) in DMF (2 mL) was added dropwise over 5 min. The mixture was stirred at 95 °C for 8 h and then stirred at rt for 16 h. The reaction mixture was poured over ice and then concentrated under reduced pressure. The residue was extracted into EtOAc (20 mL) and sequentially washed with water (10 mL), saturated aqueous $NaHCO_3$ (2 × 10 mL), water (2 × 10 mL), and brine (2 × 10 mL). The combined organic layer was dried over anhydrous Na_2SO_4, filtered, and the solvent was removed in vacuo. The residue was chromatographed on silica gel (10 g) and eluted with 30% EtOAc/haxanes to afford (*S*)-2-(4-benzylphenoxymethyl)-1-BOC-pyrrolidine (0.15 g, 73%) as a tan oil. To a solution of this product (0.12 g, 3.26 mmol) was added 4 M HCl in dioxane (15 mL) at rt . The resulting mixture was stirred overnight. The solvent was removed in vacuo to obtain an off-white solid. The solid was triturated with Et_2O to provide compound **13** (55 mg, 63%) as a white solid. MS m/z: 268 (M + H). ^{1}H NMR (400 MHz, DMSO-d_6) δ: 7.24−7.33 (m, 2H), 7.13−7.23 (m, 5H), 6.91 (d, J = 8.6 Hz, 2H), 4.16−4.26 (m, 1H), 4.09 (dd, J = 8.3, 10.47 Hz, 1H), 3.80−3.94 (m, 3H), 3.12−3.25 (m, 2H), 2.05−2.17 (m, 1H), 1.82−2.03 (m, 2H), 1.63−1.80 (m, 1H). HPLC-1: 99.4%, t_R = 15.1 min.

(*R*)-2-(4-Benzylphenoxymethyl)pyrrolidine (14). Similar to the preparation of compound **13**, the (*R*)-BOC-intermediate was prepared from 4-benzylphenol (103 mg, 0.56 mmol), NaH (19 mg, 0.75 mmol) in 1 mL DMF and (*R*)-tosylate **30** (200 mg, 0.56 mmol) in DMF (3 mL) to provide after aqueous workup a crude product which following purification by silica gel (10 g) using 30% EtOAc/hexanes as eluent provided the BOC-protected intermediate (150 mg, 73%) as a solid. MS m/z: 368 (M + H). ^{1}H NMR (400 MHz, $CDCl_3$) δ: 1.46 (m, 9H), 1.84−2.03 (m, 4H), 3.39 (m, 2H), 3.73−3.93 (m, 3H), 4.10 (m, 2H), 6.84 (m, 2H), 7.08 (m, 2H), 7.17 (m, 2H), 7.26 (m, 3H). HPLC-1: 99.8% To a solution of the BOC-protected intermediate (0.12 g) in dioxane (2 mL) was added 4N HCl in dioxane (8 mL) at rt and the resulting mixture was stirred for 1 h at rt. The solvent was removed in vacuo to obtain a thick oil. The oil was triturated with Et_2O to obtain a white solid (2.5 g). The solid was recrystallized with toluene (20 mL) to obtain the title product (58 g, 53%) as a crystalline solid (**14**). MS: m/z 268 (M + H). ^{1}H NMR (400 MHz, DMSO-d_6) δ: 7.15−7.20 (m, 5H), 7.27 (m, 2H), 6.91 (d, 2H, J = 6.8 Hz), 4.19 (dd, 1H, J_1 = 8.8, J_2 = 3.2 Hz), 4.13 (dd, 1H, J_1 = 7.2 Hz, J_2 = 6.4 Hz), 3.88 (s, 2H), 3.87 (m, 1H), 3.18 (m, 2H), 2.09 (m, 1H), 1.98 (m, 1H), 1.89 (m, 1H), 1.73 (m, 1H). HPLC-1: 98.8%, t_R = 15.2 min.

(*R*)-2-[4-(4-Thiophen-3-yl-benzyl)phenoxymethyl]pyrrolidine (15). To an argon purged solution of **35** (9.0 g, 34 mmol) and (*R*)-2-(toluene-4-sulfonyloxymethyl)pyrrolidine-1-carboxylic acid *tert*-butyl ester (12.6 g, 36 mmol) in DMF at 0 °C was added NaH (60% dispersion in mineral oil, 1.62 g, 40 mmol). The reaction was stirred at 0 °C for 10 min and warmed to 85 °C for 16 h. The reaction mixture was poured into aqueous $NaHCO_3$ (500 mL) and extracted with EtOAc (3 × 150 mL). The organic

layer was washed with water (3 × 50 mL) and dried over anhydrous $MgSO_4$. The volatiles were removed and the residue was stirred with 4N HCl in dioxane (40 mL) for 16 h. The mixture was diluted with THF (450 mL). The resulting solids were filtered and rinsed with Et_2O to give the compound **15** (7.0 g, 53%). MS *m/z*: 351 (M + H). ^{1}H NMR (400 MHz, DMSO-d_6) δ: 7.79 (d, J = 1.61 Hz, 1H), 7.58−7.66 (m, 3H), 7.51 (dd, J = 1.0, 5.0 Hz, 1H), 7.15−7.27 (m, 4H), 6.92 (d, J = 8.5 Hz, 2H), 4.20 (d, J = 3.6 Hz, 1H), 4.08 (s, 1H), 3.90 (s, 3H), 3.12−3.25 (m, 2H), 2.05−2.19 (m, 1H), 1.82−2.04 (m, 2H), 1.64−1.80 (m, 1H). HPLC-1: 99.9%, t_R = 21.0 min. Anal. calcd ($C_{22}H_{23}NOS$): C, H, N.

4-{(*R*)-2-[4-(4-Chlorobenzyl)phenoxymethyl]pyrrolidin-1-yl}-butyric Acid (16). The methyl ester **38** (0.5 g, 1.25 mmol) was dissolved in 20% water in MeOH (6 mL). Aqueous NaOH (1N, 3.5 mL) was added, and the reaction mixture was heated to 50 °C for 16 h. The solvents were removed in vacuo and the residue dissolved in water (15 mL). The pH of the solution was adjusted to ∼6−7 with 1N aqueous HCl and extracted with EtOAc (100 mL). The organic layer was separated, dried over anhydrous $MgSO_4$, and the solvent was removed in vacuo to give the compound **16** (0.42 g, 87%). MS *m/z*: 388 (M + H). ^{1}H NMR (400 MHz, DMSO-d_6) δ: 7.32 (d, J = 8.3 Hz, 2H), 7.22 (d, J = 8.3 Hz, 2H), 7.11 (d, J = 8.5 Hz, 2H), 6.84 (d, J = 8.5 Hz, 2H), 3.82−3.90 (m, 3H), 3.72 (dd, J = 6.7, 9.5 Hz, 1H), 3.00−3.09 (m, 1H), 2.74−2.90 (m, 2H), 2.36 (ddd, J = 5.2, 6.8, 12.0 Hz, 1H), 2.14−2.30 (m, 3H), 1.91 (dd, J = 8.3, 12.0 Hz, 1H), 1.52−1.75 (m, 5H). HPLC-1: 98.2%, t_R = 20.2 min.

(*R*)-2-[4-(4-Chlorophenoxy)phenoxymethyl]pyrrolidine Hydrochloride (17). Compound **41** was prepared from **30** analogous to the procedure described for **40** as a yellow oil (0.37 g). ^{1}H NMR (400 MHz, DMSO-d$_6$) δ: 7.38 (d, J = 8.8 Hz, 2H), 7.00 (s, 4H), 6.93 (d, J = 8.8 Hz, 2H), 4.02 (br s, 2H), 3.83−3.93 (m, 1H), 3.27 (br s, 2H), 1.86−2.02 (m, 3H), 1.76−1.84 (m, 1H), 1.40 (s, 9H).

A solution of 4N HCl in *p*-dioxane (5 mL) was added to **41** (0.36 g, 0.89 mmol). The resulting mixture was stirred at rt for 2 h. The solvent was removed in vacuo. The crude product was triturated with Et_2O and dried in vacuo to afford the compound **17** (0.19 g, 70%) as a light-yellow solid. ^{1}H NMR (400 MHz, DMSO-d_6) δ: 1.75 (m, 1H), 1.87−2.01 (m, 2H), 2.12 (m, 1H), 3.21 (m, 2H), 3.89 (m, 1H), 4.17 (m, 1H), 4.24 (dd, J = 4.0, 10.8 Hz, 1H), 6.94 (d, J = 9.2 Hz, 2H), 7.05 (s, 4H), 7.40 (d, J = 8.8 Hz, 2H). LCMS *m/z*: 304.2 (M + l). HPLC-1: (99.1%), t_R = 19.2 min. Anal. calcd ($C_{17}H_{18}ClNO_2 \cdot HCl$): C, H, N.

3-{(*R*)-2-[4-(4-Chlorophenoxy)phenoxymethyl]pyrrolidin-1-yl}-propionic Acid Hydrochloride (18). A solution of **46** (0.62 g, 1.59 mmol) in 1:1 conc. HCl/*p*-dioxane (26 mL) was stirred at 60 °C for 4 h. The solvent was removed in vacuo. The crude product was triturated with ether and the solvent was removed in vacuo to afford the title compound **18** (0.40 g, 68%) as a white solid. MS *m/z*: 374.5 (M − 1). ^{1}H NMR (400 MHz, DMSO-d_6) δ: 1.83 (m, IH), 2.00 (m, 2H), 2.24 (m, IH), 2.86 (m, 2H), 3.18 (m, IH), 3.38 (m, IH), 3.63 (m, 2H), 3.96 (m, IH), 4.28−4.37 (m, 2H), 6.94 (d, J = 9.2 Hz, 2H), 7.06 (s, 4H), 7.39 (d, J = 8.8 Hz, 2H). HPLC-1: 97.7%, t_R = 19.5 min.

4-{(*R*)-2-(4-(4-Chlorophenoxy)phenoxymethyl)pyrrolidin-1-yl}-l-butyric Acid Hydrochloride (19). A solution of the methyl ester **47** (0.8 g, 1.99 mmol) in conc. HCl (18 mL) and *p*-dioxane (18 mL) was stirred at 60 °C for 4 h. The solvent was removed in vacuo to provide an oil. The oil was triturated with Et_2O (10 mL), and the resulting solid was filtered to yield the title compound **19** (0.72 g, 93%) as a white solid. MS *m/z*: 388 (M − 1). ^{1}H NMR (400 MHz, DMSO-d_6) δ: 1.82−2.03 (m, 5H), 2.24 (m, 1H), 2.38 (t, J = 7.2 Hz, 2H), 3.15 (m, 2H), 3.49 (m, 1H), 3.64 (m, 1H), 3.90 (m, 1H), 4.28−4.34 (m, 2H), 6.94 (d, J = 9.2 Hz, 2H), 7.06 (s, 4H), 7.40 (d, J = 8.8 Hz, 2H). HPLC-2: 98.1%, t_R = 18.5 min.

4-{(*S*)-2-[4-(4-Chlorophenoxy)phenoxymethyl]pyrrolidin-1-yl}-butyric Acid Hydrochloride (20). To a solution of **48** (2.2 g, 5.45 mmol) in MeOH (22 mL) was added 2N aqueous NaOH (7.2 mL, 14.5 mmol). The resulting solution was stirred at rt overnight. The solvent was removed in vacuo. The crude oil was dissolved in water (45 mL), and the pH was adjusted to 7 with 2N HCI solution. The crude residue was extracted into EtOAc (3 × 250 mL). The combined organic portions were washed with brine, dried over anhydrous Na_2SO_4, filtered, and the solvent was removed in vacuo. The crude product was purified by silica gel flash chromatography using (0−20% MeOH/CH_2Cl_2, gradient) to give the free base of the title compound as a yellow oil. To the oil was added 2 M HCI in Et_2O (35 mL). The resulting mixture was stirred at rt for 2 h. After removal of the supernatant solvent, the remaining white solid was triturated in Et_2O (50 mL) for 1 h. The slurry was filtered, washed with Et_2O (3 × 25 mL), and dried at 45 °C for 48 h to afford the title compound **20** (0.84 g, 36%) as a white solid. ^{1}H NMR (400 MHz, DMSO-d_6) δ: 1.82−2.03 (m, 5H), 2.23 (m, 1H), 2.38 (t, J = 7.2 Hz, 2H), 3.14 (m, 2H), 3.48 (m, 1H), 3.63 (m, 1H), 3.90 (m, 1H), 4.28−4.37 (m, 2H), 6.94 (d, J = 8.8 Hz, 2H), 7.06 (s, 4H), 7.40 (d, J = 8.8 Hz, 2H), 10.55 (br, 1H), 12.30 (br, 1H). HPLC-1: 99.5%, t_R = 19.5 min. Anal. calcd ($C_{21}H_{24}ClNO_4 \cdot$ HCl): C, H, N.

4-(4-Phenoxyphenyl)piperazine-1-carboxylic Acid *tert*-Butyl Ester (25). nBu_3P (0.7 g . 3.0 mmol), $Pd_2(dba)_3$ (0.36 g, 0.3 mmol), and NaOtBu (1.26 g, 13.1 mmol) were added to a solution of **23** (3.9 g, 13.1 mmol) and 1-BOC-piperazine (2.5 g, 13.1 mmol) in toluene (20 mL). The reaction mixture was stirred at rt overnight and then filtered. The solvent was removed in vacuo, and the residue was purified on silica gel (70 g) using 1% MeOH in CH_2Cl_2 to yield the title compound **25** (3.5 g, 75.5%) as a light-yellow solid. MS *m/z*: 355 (M + H). LCMS 99%. ^{1}H NMR (400 MHz, $CDCl_3$) δ: 7.57 (d, J = 8.9 Hz, 2 H) 6.89−6.98 (m, 4 H) 6.71 (d, J = 8.9 Hz, 2 H) 3.55−3.62 (m, 4 H) 3.05−3.11 (m, 4 H) 1.49 (s, 9H).

4-[4-(4-Iodophenoxy)phenyl]piperazine-1-carboxylic Acid *tert*-Butyl Ester (26). To a solution of **24** (4.22 g 10 mmol), 1-BOC-piperazine (1.86 g, 10 mmol) were added $Pd_2(dba)_3$ (0.270 g, 0.295 mmol), nBu_3P (0.58 g, 2.8 mmol), and NaOtBu (0.95 g, 10 mmol). The reaction mixture was stirred at rt overnight and then filtered. The solvent was removed in vacuo, and the residue was purified on silica gel (100 g) using 1% MeOH in CH_2Cl_2 to yield the title compound **26** (1.2 g, 25%) as a yellow solid. MS *m/z*: 481 (M + H), LCMS 97%. ^{1}H NMR (400 MHz, $CDCl_3$) δ: 7.57 (d, J = 8.9 Hz, 2 H), 6.93 (dd, J = 16.0, 9.4 Hz, 4 H), 6.71 (d, J = 8.7 Hz, 2 H), 3.55−3.61 (m, 4 H), 3.05−3.12 (m, 4 H), 1.49 (s, 9H).

(*S*)-2-(Toluene-4-sulfonyloxymethyl)pyrrolidine-1-carboxylic Acid *tert*-Butyl Ester (29). To a solution of (*S*)-*N*-BOC-prolinol (22 g, 110 mmol) in pyridine (56 mL) at 0 °C was added a solution of *p*-toluenesulfonyl chloride (22.9 g, 120 mmol) in pyridine (56 mL) portionwise over 5 min. The pale-yellow reaction mixture was stirred at 0 °C for 2 h and then at rt overnight. The solvent was removed in vacuo. The crude oil was extracted into EtOAc (400 mL) and sequentially washed with 0.5 M HCl (100 mL), saturated aqueous $NaHCO_3$ (100 mL), and brine (100 mL). The combined organic layer was dried over anhydrous Na_2SO_4, filtered, and the solvent was removed in vacuo to give compound **27** (39 g, 99%) as a yellow oil. MS *m/z*: 356 (M + H). ^{1}H NMR (400 MHz, $CDCl_3$) δ: 7.79 (d, J = 8.1 Hz, 2H), 7.31−7.40 (m, 2H), 4.06−4.18 (m, 2H), 3.90 (br s, 1H), 3.30 (d, J = 6.3 Hz, 2H), 2.45 (s, 3H), 1.74−2.00 (m, 4H), 1.39 (d, J = 16.4 Hz, 9H).

(*R*)-2-(Toluene-4-sulfonyloxymethyl)pyrrolidine-1-carboxylic Acid *tert*-Butyl Ester (30). This compound was prepared analogously to the preparation of **29** from (*R*)-BOC-prolinol **28** (500 mg, 2.48 mmol) and tosyl chloride (565 mg, 2.96 mmol) in pyridine (2.5 mL) to provide, after aqueous workup and concentration of organic solvent in vacuo, the tosylate **30** (800 mg, 91%) as a thick oil. MS *m/z*: 378 (M + Na). ^{1}H NMR (400 MHz, $CDCl_3$) δ: 1.38 (m, 9H), 1.79 (m, 2H), 1.93 (m, 2H), 2.44 (s, 3H),

3.26−3.32 (m, 3H), 3.88−3.97 (m, 2H), 4.07−4.14 (m, 2H), 7.34 (br, 2H), 7.77 (d, 2H, J = 8.0 Hz).

(4-Chlorophenyl)(4-methoxyphenyl)methanone (32a). Prepared according to the procedure for **32b** from 4-chlorobenzoyl chloride. ^{1}H NMR (400 MHz, $CDCl_3$) δ: 7.80 (d, J = 8.7 Hz, 2H), 7.71 (d, J = 8.5 Hz, 2H), 7.45 (d, J = 8.5 Hz, 2H), 6.97 (d, J = 8.7 Hz, 2H), 3.89 (s, 3H).

(4-Iodophenyl)(4-methoxyphenyl)methanone (32b). Cold nitrobenzene (45 mL) was treated portionwise with $AlCl_3$ (13.5 g, 101 mmol). 4-Iodobenzoyl chloride **31b** (25 g, 94 mmol) in nitrobenzene (20 mL) was added, keeping the reaction temperature at < 10 °C. The mixture was stirred at 0 °C for 10 min, and anisole (9.5 g, 88 mmol) was added dropwise to maintain temperature at < 10 °C. The reaction was allowed to rt over 16 h and then poured into ice water (750 mL). The resulting solids were removed by filtration, and the filtrate was extracted with CH_2Cl_2 (2 L). The organic materials were washed with $NaHCO_3$ (2 × 150 mL), dried over anhydrous $MgSO_4$, and the solvent was removed in vacuo. The residue was triturated with cyclohexane (200 mL) to obtain **32b** as a solid (26.75 g, 90%). ^{1}H NMR (400 MHz, $CDCl_3$) δ: 7.84 (d, J = 8.3 Hz, 2H), 7.80 (d, J = 8.9 Hz, 2H), 7.48 (d, J = 8.3 Hz, 2H), 6.96 (d, J = 8.9 Hz, 2H), 3.89 (s, 3H).

4-(4-Chlorobenzyl)methoxybenzene (33b). A solution of **32b** (9.8 g, 39.7 mmol) in TFA (30 mL) was cooled to 0 °C. To this solution was added triethylsilane (19.22 g, 164.7 mmol), and the reaction was allowed to rt for 16 h. The reaction was poured into water (150 mL) and was adjusted to pH 6−7 with 1N NaOH. The solution was extracted with EtOAc (400 mL), and the organic layer was washed with water (200 mL) and then dried over anhydrous $MgSO_4$. The solvent was removed in vacuo to give the title product **33b** (9.2 g, 99%), which was used without further purification for the next step. ^{1}H NMR (400 MHz, $CDCl_3$) δ: 7.25 (d, J = 3.9 Hz, 2H), 7.09 (d, J = 8.4 Hz, 2H), 7.07 (d, J = 8.4 Hz, 2H), 6.83 (d, J = 8.6 Hz, 2H), 3.88 (s, 2H), 3.78 (s, 3H).

4-(4-Chlorobenzyl)phenol (34a). Prepared according to the procedure for **34b** starting with 4-(4-chlorobenzyl)methoxybenzene. ^{1}H NMR (400 MHz, $CDCl_3$) δ: 7.30 (d, J = 3.4 Hz, 2H), 7.13 (d, J = 8.3 Hz, 2H), 7.06 (d, J = 8.5 Hz, 2H), 6.80 (d, J = 8.5 Hz, 2H), 4.74 (s, 1H), 3.91 (s, 2H).

4-(4-Iodobenzyl)phenol (34b). To a solution of **32b** (26.7 g, 79 mmol) in TFA (90 mL) at 0 °C, triethylsilane (29 mL, 181 mmol) was added slowly. The reaction was stirred at rt for 16 h. The volatiles were removed in vacuo. The residue was dissolved in EtOAc (200 mL), washed with $NaHCO_3$ (2 × 300 mL) and 6N HCl (2 × 50 mL), and then dried over anhydrous $MgSO_4$. Removal of solvent in vacuo gave an oil, which was used without further purification. ^{1}H NMR (400 MHz, $CDCl_3$) δ: 7.59 (d, J = 8.2 Hz, 2H), 7.06 (d, J = 8.6 Hz, 2H), 6.92 (d, J = 8.2 Hz, 2H), 6.82 (d, J = 8.6 Hz, 2H), 3.85 (s, 2H), 3.78 (s, 3H). To a −78 °C. solution of crude **33b** in CH_2Cl_2 (150 mL) was added BBr_3 (1 M in CH_2Cl_2, 158 mL, 158 mmol) while maintaining the reaction temperature below −65 °C. The reaction was allowed to come to rt, then quenched by pouring over ice water (1 L). The aqueous material was extracted with CH_2Cl_2 (2 × 100 mL). The organic layer was washed with $NaHCO_3$ (2 × 2000 mL) and brine (100 mL) and then dried over anhydrous $MgSO_4$. The solvent was removed in vacuo, and the residue triturated with hexanes to obtain the product **34b** (22.3 g, 91%). ^{1}H NMR (400 MHz, $CDCl_3$) δ: 7.59 (d, J = 8.2 Hz, 2H), 7.01 (d, J = 8.3 Hz, 2H), 6.91 (d, J = 8.2 Hz, 2H), 6.75 (d, J = 8.5 Hz, 2H), 4.68 (s, 1H), 3.84 (s, 2H).

4-(4-Thiophen-3-yl-benzyl)phenol (35). A mixture of **34b** (12.4 g, 40 mmol), 3-thienylboronic acid (6.15 g, 48 mmol), Pd/C (2.12 g, 2 mmol), and K_2CO_3 (16.6 g, 120 mmol) was suspended in IPA/H_2O (5:1, 240 mL) under an argon purge. The stirred mixture was heated at 85 °C for 16 h. After cooling to rt, the reaction was passed through a pad of celite and concentrated in vacuo. The residue was triturated with water and the solids were isolated by filtration to give the title product **35** (10.6 g, 99%). ^{1}H NMR (400 MHz, $CDCl_3$) δ: 7.51 (d, J = 8.1 Hz, 2H), 7.39−7.43 (m, 1H), 7.36 (d, J = 2.2 Hz, 2H), 7.19 (d, J = 8.1 Hz, 2H), 7.07 (d, J = 8.3 Hz, 2H), 6.76 (d, J = 8.5 Hz, 2H), 4.68 (s, 1H), 3.93 (s, 2H).

(*R*)-2-[4-(4-Chlorobenzyl)phenoxymethyl]pyrrolidine (37). Synthesis was carried out analogous to procedure used for the preparation of **15** starting with **34a**. BOC protected intermediate, (*R*)-2-[4-(4-chlorobenzyl)-phenoxymethyl]-pyrrolidine-1-carboxylic acid *tert*-butyl ester, was purified by flash column chromatography (15% EtOAc/hexanes, isocratic). ^{1}H NMR (400 MHz, $CDCl_3$) δ: 7.23 (d, J = 8.2 Hz, 2H), 7.09 (d, J = 8.3 Hz, 2H), 7.05 (d, J = 8.1 Hz, 2H), 6.85 (d, J = 6.5 Hz, 2H), 4.04−4.21 (m, 2H), 3.87 (s, 2H), 3.68−3.81 (m, 1H), 3.27−3.46 (m, 2H), 1.78−2.03 (m, 4H), 1.46 (s, 9H).

4-{(*R*)-2-[4-(4-Chlorobenzyl)phenoxymethyl]pyrrolidin-1-yl}-butyric Acid Methyl Ester (38). A solution of **37** (1.6 g, 4 mmol) was treated with 4 N HCl in *p*-dioxane (25 mL) for 6 h at rt, the solvent was removed in vacuo, and residue dried under high vacuum for 4 h to provide solid (1.4 g) that was used as such for the next step. To solid (1.4 g, 4 mmol) and methyl-4-bromobutyrate (0.9 g, 5 mmol) in DMF (15 mL) was added K_2CO_3 (1.1 g, 8 mmol). The reaction mixture was stirred at rt for 16 h. The solvent was removed in vacuo, and the residue was partitioned between water (35 mL) and EtOAc (130 mL). The organic layer was dried over anhydrous $MgSO_4$, the solvent was removed in vacuo, and residue was purified by flash chromatography (50% EtOAc/hexanes, isocratic) to give the ester **38** (0.57 g, 35%). ^{1}H NMR (400 MHz, $CDCl_3$) δ: 7.25 (d, J = 6.6 Hz, 2H), 7.09 (d, J = 8.3 Hz, 2H), 7.05 (d, J = 8.6 Hz, 2H), 6.82 (d, J = 8.6 Hz, 2H), 3.86−3.92 (m, 3H), 3.74 (dd, J = 6.9, 9.1 Hz, 1H), 3.64 (s, 3H), 3.15 (d, J = 4.0 Hz, 1H), 2.79−2.92 (m, 2H), 2.30−2.47 (m, 3H), 2.24 (q, J = 8.3 Hz, 1H), 1.96 (d, J = 11.8 Hz, 1H), 1.63−1.88 (m, 5H).

(*S*)-2-(4-Iodophenoxymethyl)pyrrolidine-1-carboxylic Acid *tert*-Butyl Ester (40). To a solution of 4-iodophenol (24.2 g, 110 mmol) in DMF (200 mL) was added KOtBu (12.3 g, 110 mmol). The cloudy solution was stirred at rt for 30 min before a solution of **29** (35.9 g, 100 mmol) in DMF (200 mL) was added. The reaction was heated to 45 °C for 16 h and then increased to 55 °C for 8 h. The solvent was removed in vacuo, and the residue was partitioned between hexanes (500 mL) and water (250 mL). The organic layer was washed with 0.2 N NaOH (2 × 200 mL) and H_2O (250 mL). The solvent was reduced to 20% and allowed to stand at rt for 1 h. The supernatant liquid was decanted, and the remaining solids were washed with hexane (50 mL). The solid was dried under high vacuum at rt to give the title compound **40** (37.0 g, 92%). ^{1}H NMR (400 MHz, DMSO-d_6) δ: 7.58 (d, J = 8.7 Hz, 2H), 6.82 (d, J = 8.8 Hz, 2H), 3.95−4.07 (m, 2H), 3.82−3.93 (m, 1H), 3.26 (br. s., 2H), 1.71−2.03 (m, 4H), 1.39 (s, 9H).

(*S*)-2-[4-(4-Chlorophenoxy)phenoxymethyl]pyrrolidine-1-carboxylic Acid *tert*-Butyl Ester (42). A mixture of **40** (11.8 g, 29.3 mmol), 4-chlorophenol (11.3 g, 87.9 mmol), copper(I) iodide (1.4 g, 7.3 mmol), cesium carbonate (38.2 g, 117.2 mmol), and *N*, *N*-dimethylglycine (1.5 g, 14.6 mmol) in *p*-dioxane (200 mL) was heated to reflux under an N_2 atmosphere for 16 h. The reaction mixture was concentrated in vacuo, and residue was partitioned between hexanes (500 mL) and water (250 mL). The organic layer was washed with 0.2N NaOH (2 × 250 mL) and water (250 mL) and then concentrated in vacuo to give a crude oil. The oil was purified by silica gel flash chromatography (10% acetone/hexanes, isocratic) to give the title compound **42** (6.6 g, 56%). MS m/z: 404 (M + H). ^{1}H NMR (400 MHz, DMSO-d_6) δ: 7.38 (d, J = 8.8 Hz, 2H), 7.00 (s, 4H), 6.93 (d, J = 8.8 Hz, 2H), 3.96−4.09 (m, 2H), 3.83−3.94 (m, 1H), 3.27 (br. s., 2H), 1.86−2.04 (m, 3H), 1.74−1.85 (m, 1H), 1.40 (s, 9H).

(*S*)-2-[4-(4-Chlorophenoxy)phenoxymethyl]pyrrolidine (43). Compound **42** (6.6 g, 16.4 mmol) was stirred in 4 N HCl in *p*-dioxane at rt for 2 h. The solvent was removed in vacuo, and

the residue was partitioned between hexanes (200 mL) and water (200 mL). The organic layer was extracted with 1 N HCl (25 mL). The aqueous layers were combined, neutralized with Na_2CO_3 (solution), and extracted with hexanes (2 × 100 mL). The solvent was removed in vacuo at 40 °C until the solution became cloudy. The mixture was allowed to stand at rt and then refrigerated for 1 h. The supernatant liquid was decanted, and the resulting solids were dried under vacuum at rt to give the title compound **43** (4.1 g, 83%). ^{1}H NMR (400 MHz, DMSO-d_6) δ: 7.38 (d, J = 8.7 Hz, 2H), 6.87−7.05 (m, 6H), 3.73−3.84 (m, 2H), 3.26−3.43 (m, 1H), 2.72−2.88 (m, 2H), 2.30−2.46 (m, 1H), 1.78−1.92 (m, 1H), 1.54−1.76 (m, 2H), 1.35−1.52 (m, 1H).

Methyl 3-[(2*R*)-2-{[4-(4-Chlorophenoxy)phenoxy]methyl}-1-pyrrolidinyl]propanoate (46). To a solution of (**17**) (0.8 g, 2.63 mmol) in CH_2Cl_2 (7.6 mL) was added Et_3N (0.78 mL, 5.60 mmol) and methyl 3-bromopropionate (0.32 mL, 2.93 mmol). The resulting solution was stirred at 30 °C overnight. The reaction mixture was poured into water/CH_2Cl_2 (50 mL/50 mL). The crude residue was extracted into CH_2Cl_2 (50 mL). The organic portion was washed with water (50 mL), washed with brine (50 mL), dried over anhydrous Na_2SO_4, filtered, and concentrated in vacuo. The crude product was purified by silica gel flash chromatography (0−50% EtOAc/hexanes, gradient) to give the title compound **46** (0.79 g, 77%). ^{1}H NMR (400 MHz, DMSO-d_6) δ: 7.34−7.42 (m, 2H), 6.90−7.04 (m, 6H), 3.90 (dd, J = 5.1, 9.4 Hz, 1H), 3.74 (dd, J = 6.5, 9.5 Hz, 1H), 3.57 (s, 3H), 3.15 (d, J = 12.2 Hz, 1H), 2.98−3.06 (m, 1H), 2.83 (dd, J = 5.9, 8.1 Hz, 1H), 2.56−2.66 (m, 1H), 2.38−2.48 (m, 2H), 2.23 (d, J = 7.9 Hz, 1H), 1.85−1.98 (m, 1H), 1.65−1.76 (m, 2H), 1.59 (s, 1H).

4-{(*R*)-2-(4-(4-Chlorophenoxy)phenoxymethyl)pyrrolidin-1-yl}-l-butyric Acid Methyl Ester (47). To a solution of **17** (0.8 g, 2.63 mmol) in CH_2Cl_2 (7.6 mL) was added Et_3N (0.78 mL, 5.60 mmol) and methyl 4-bromobutyate (0.35 mL, 3.04 mmol). The resulting solution was stirred at 30 °C overnight. The reaction mixture was poured into water/CH_2Cl_2 (50 mL/50 mL). The crude residue was extracted into CH_2Cl_2. The organic portion was washed with water (50 mL), brine (50 mL), dried over anhydrous Na_2SO_4, filtered, and concentrated in vacuo. The crude product was purified by silica gel flash chromatography using (0−50% EtOAc/hexanes, gradient) to give the methyl ester **47** (0.60 g, 57%). ^{1}H NMR (400 MHz, DMSO-d_6) δ: 7.38 (d, J = 8.8 Hz, 2H), 6.89−7.03 (m, 6H), 3.87 (dd, J = 5.0, 9.5 Hz, 1H), 3.73 (dd, J = 6.6, 9.4 Hz, 1H), 3.55 (s, 3H), 2.98−3.08 (m, J = 3.6 Hz, 1H), 2.81−2.89 (m, J = 12.0 Hz, 1H), 2.73−2.81 (m, J = 1.9 Hz, 1H), 2.29−2.40 (m, 3H), 2.17 (q, J = 7.9 Hz, 1H), 1.85−1.98 (m, 1H), 1.63−1.77 (m, 4H), 1.53−1.63 (m, 1H).

4-{(*S*)-2-[4-(4-Chlorophenoxy)phenoxymethyl]pyrrolidin-1-yl}-butyric Acid Methyl Ester (48). To a solution of **43** (4.0 g, 13.2 mmol) in DMF (50 mL) was added K_2CO_3 (3.7 g, 26.5 mmol) and methyl 4-bromobutyrate (3.6 g, 19.8 mmol). The resulting suspension was stirred at 55 °C for 16 h. The solvent was removed in vacuo, and the residue was partitioned between hexanes (250 mL) and water (150 mL). The organic layer was washed with water (150 mL), dried over anhydrous Na_2SO_4, filtered, and concentrated in vacuo. The crude product was purified by silica gel flash chromatography (1−2% iPrOH/EtOAc + 0.25% TEA, gradient) to give the title compound **48** (4.1 g, 77%). MS m/z: 404 (M + H). ^{1}H NMR (400 MHz, DMSO-d_6) δ: 7.38 (d, J = 8.8 Hz, 2H), 6.89−7.03 (m, 6H), 3.87 (dd, J = 5.1, 9.4 Hz, 1H), 3.73 (dd, J = 6.7, 9.3 Hz, 1H), 3.55 (s, 3H), 3.00−3.08 (m, 1H), 2.73−2.90 (m, 2H), 2.30−2.40 (m, 3H), 2.17 (q, J = 8.2 Hz, 1H), 1.85−2.01 (m, 1H), 1.64−1.76 (m, 4H), 1.60 (q, J = 6.0 Hz, 1H).

Biological Assays. In Vitro Enzyme Assay. LTA_4 substrate was prepared from the methyl ester of LTA_4 (BioMol, Plymouth Meeting, PA, or Cayman Chemicals, Ann Arbor, MI) by treatment under nitrogen with 100 mol equiv of NaOH in an acetone:H_2O (4:1) solution at rt for 40 min. Stock solutions of LTA_4 were kept frozen at −80 °C for a maximum of one week prior to use.

Recombinant human LTA_4H (200 nM) was incubated with various concentrations of test compound for 10 min at rt in assay buffer (0.1 M Tris-HCl, 0.1 M NaCl, 5 mg/mL fatty acid free BSA, 10% DMSO, pH 8.0). Immediately before the assay, LTA_4 was diluted to a concentration of 10 μM in assay buffer (without DMSO) and added to the reaction mixture to a final concentration of 2 μM to initiate the enzyme reaction. Samples were incubated for 2 min at rt, followed by the addition of 2 volumes of chilled quenching buffer (CH_3CN with 1% HOAc and 225 nM LTB_4-d_4 (BioMol)). The samples were then stored at 4 °C overnight to complete protein precipitation and centrifuged for 15 min at 1800g. LTB_4 formed was measured in the supernatant by LC-MS/MS using LTB_4-d_4 as an internal standard and an external LTB_4 standard (BioMol) for a calibration curve. Briefly, the analyte was separated from LTB_4 isomers formed by spontaneous hydrolysis of LTA_4 using isocratic elution on an HPLC system (Waters, Milford, MA) and analyzed on a tandem quadrupole mass spectrometer (Waters Micromass Quattro Premier). MRM transitions followed on 2 channels were 335.2 → 195.3 (LTB_4) and 339.2 → 197.3 (LTB_4-d_4). On the basis of the measured amounts of LTB_4 formed at each inhibitor concentration, a dose−response curve was fitted to the data using a sigmoidal 4-parameter function (XLfit, model 205) and an IC_{50} value was calculated.

Human Whole Blood LTB_4 Assay. Human blood (45 mL) was collected in heparin-containing Vacutainer tubes (Greiner-Bio One) with informed consent. Individual experiments were performed with blood from a single subject. For each sample, 200 μL of blood were dispensed into a prewarmed 96-well plate and 188 μL of RPMI-1640 medium (Invitrogen) containing 20 μg/mL Indomethacin (Sigma, St. Louis, MO) was added. Then 4 μL of a series of compound dilutions (final DMSO concentration of 1%) were added in triplicate, followed by a 15 min incubation at 37 °C with gentle shaking. After that, blood samples were stimulated by adding 8 μL of ionomycin (from *Streptomyces conglobatus*, Calbiochem) to a final concentration of 36 μM. After another incubation at 37 °C for 30 min, samples were centrifuged at 4 °C for 5 min at 1800g. LTB_4 concentrations in supernatants were determined using a commercially available enzyme-linked immunosorbent assay (R&D Systems, Minneapolis, MN) according to the manufacturer's instructions. On the basis of the measured amounts of LTB_4 formed at each inhibitor concentration, a dose−response curve was fitted to the data using a sigmoidal three-parameter function (XLfit, model 203 with Hill slope fixed to −1) and an IC_{50} value was calculated. Each assay plate contained eight positive controls (no compound) and eight negative controls (no ionomycin).

X-ray Crystallography. With PEG8000 as precipitant, ytterbium as an additive, and the use of microseeding to control nucleation rate, well-diffracting crystals of the enzyme in complex with the micromolar inhibitor Bestatin were obtained routinely. These crystals were subsequently used to soak in various high-affinity lead compounds of interest, replacing Bestatin. Using this strategy, a crystal structure of LTA_4H in complex with compounds **2**, **5**, **6**, **7**, **8**, **9**, **13**, **14**, **15**, and **20** were determined at 1.67, 2.16, 1.8, 2.0, 2.05, 2.4, 1.90, 1.6, 1.63, and 2.5 Å resolution, respectively. The carboxylate group of compound **20** chelates the catalytic Zn ion, its oxygens replacing two water oxygens in almost identical positions in the structure with compound **14**. The two phenyl rings of both compounds bind in a very similar mode to the end of the bend, hydrophobic substrate binding pocket, which has three conserved waters tightly bound.

Oral Dosing of Compounds to Rats. The compound was formulated in 10% Solutol HS15 (BASF AG, Ludwigshafen, Germany), 30 mM NaH_2PO_4, pH 7.9. The same solution without the compound was used for vehicle control experiments. The

solutions were given by orogastric gavage to male Sprague−Dawley rats in a dosing volume of 10 mL/kg (1% of body weight) using stainless steel feeding needles of 0.9 mm × 38 mm (B & K Universal AB, Sollentuna, Sweden) and 1 mL Omnifix syringes (B. Braun, Melsungen, Germany). The rats were fasting in the single dose time course experiments and nonfasting in all the other experiments.

Isolation of Whole Blood from Dosed Animals. Rats were put in a special cylinder to hold them still. The tail vein was punctured with 25G × 5/8 in. needle and the blood collected into a heparin tube. Dosing in dog and monkey was carried out at CROs sites.

Acknowledgment. We wish to acknowledge technical contributions of Jenny Lin for providing guidance and overall analytical support, Denise Anderson for running mass spectral analyses, Dr. Nelson Zhao for acquiring NMR spectra, and Brian Pease for generating analytical HPLC data. We also thank Dr. Kari Stefansson for helpful discussions and encouragement during the course of this work.

Supporting Information Available: Elaboration of fragments, hydrophilic linkers for which bound-structures are shown, hydrolase-bound fragments containing hydrophilic linkers, plot of BEI vs. SEI, preparation of recombinant human LTA_4 hydrolase, protein crystallization, preparation of compound-soaked crystals and crystal freezing, and data collection, structure solution, and refinement. This material is available free of charge via the Internet at http://pubs.acs.org.

References

(1) Helgadottir, A.; Manolescu, A.; Thorleifsson, G.; Jonsdottir, H.; Thorsteinsdottir, U.; Samani, N. J.; Gretarsdottir, S.; Johannsson, H.; Gudmundsson, G.; Grant, S. F. A.; Sveinbjornsdottir, S.; Valdimarsson, E. M.; Matthiasson, S. E.; Gudmundsdottir, O; Gurney, M.; Sainz, J.; Thorhallsdottir; Andresdottir, M.; Frigge, M. L.; Gudnason, V.; Kong, A.; Topol, E. J.; Thorgeirsson, G.; Gulcher, J. R.; Hakonarson, H.; Stefansson, K. The gene encoding 5-lipoxygenase activating protein confers risk of myocardial infarction and stroke. *Nat. Genet.* **2004**, *36*, 233–239.

(2) Helgadottir, A.; Manolescu, A.; Helgason, A.; Thorleifsson, G.; Thorsteinsdottir, U.; Gudbjartsson, D. F.; Gretarsdottir, S.; Magnusson, K. P.; Gudmundsson, G.; Hicks, A.; Jonsson, T.; Grant, S. F. A.; Sainz, J.; O'Brien, S. J.; Sveinbjornsdottir, S.; Valdimarsson, E. M.; Matthiasson, S. E.; Levey, A. I.; Abramson, J. L.; Reilly, M.; Vaccarino, V.; Wolfe, M.; Gudnason, V.; Quyyumi, A. A.; Topol, E. J.; Rader, D. J.; Thorgeirsson, G.; Gulcher, J. R.; Hakonarson, H.; Kong, A.; Stefansson, K. A variant of the gene encoding leukotriene A4 hydrolase confers ethnicity-specific risk of myocardial infarction. *Nat. Genet.* **2006**, *38*, 68–74.

(3) Meng, C. Q. Atherosclerosis is an inflammatory disorder after all. *Curr. Top. Med. Chem* **2006**, *6*, 93–102.

(4) Spanbroek, R.; Grabner, R.; Lotzer, K.; Hildner, M.; Urbach, A.; Ruhling, K.; Moos, M. P.; Kaiser, B.; Cohnert, T. U.; Wahlers, T.; Zieske, A.; Plenz, G.; Robenek, H.; Salbach, P.; Kuhn, H.; Radmark, O.; Samuelsson, B.; Habenicht, A. J. Expanding expression of the 5-lipoxygenase pathway within the arterial wall during human atherogenesis. *Proc. Natl. Acad. Sci. U.S.A.* **2003**, *100* (3), 1238–1243.

(5) Cipollone, F.; Mezzetti, A.; Fazia, M. L.; Cuccurullo, C.; Iezzi, A.; Ucchino, S.; Spigonardo, F.; Bucci, M.; Cuccurullo, F.; Prescott, S. M.; Stafforini, D. M. Association between 5-lipoxygenase expression and plaque instability in humans. *Arterioscler. Thromb. Vasc. Biol.* **2005**, *25*, 1665–1670.

(6) Qiu, H.; Gabrielsen, A.; Agardh, H. E.; Wan, M.; Wetterholm, A.; Wong, C. H.; Hedin, U.; Swedenborg, J.; Hansson, G. K.; Samuelsson, B.; Paulsson-Berne, G.; Haeggström, J. Z. Expression of 5-lipoxygenase and leukotriene A4 hydrolase in human atherosclerotic lesions correlates with symptoms of plaque instability. *Proc. Natl. Acad. Sci. U.S.A.* **2006**, *103* (21), 8161–8166.

(7) (a) Lewis, R. A.; Austen, K. F.; Soberman, R. J. Leukotrienes and other products of the 5-lipoxygenase pathway. Biochemistry and relation to pathology in human diseases. *N. Engl. J. Med.* **1990**, *232*, 645–655. (b) Drazen, J. M.; Austen, K. F. Leukotrienes and airway responses. *Am. Rev. Respir. Crit. Care Dis.* **1987**, *136*, 985–998. (c) Drazen, J. M. Pharmacology of leukotriene receptor antagonists and 5-lipoxygenase inhibitors in the management of asthma. *Pharmacotherapy* **1997**, *17*, S22–S30. (d) Marx, J. L. The leukotrienes in allergy and inflammation. *Science* **1982**, *215*, 1380–1383. (e) Griffiths, R. J.; Pettipher, E. R.; Koch, K.; Farrell, C. A.; Breslow, R.; Conklyn, M. J.; Smith, M. A.; Hackman, B. C.; Wimberly, D. J.; Milici, A. J. Leukotriene B4 plays a critical role in the progression of collagen-induced arthritis. *Proc. Natl. Acad. Sci. U.S.A.* **1995**, *92* (2), 517–521. (f) Shao, W. H.; Del, Prete, A.; Bock, C. B.; Haribabu, B. Targeted disruption of leukotriene B4 receptors BLT1 and BLT2: a critical role for BLT1 in collagen-induced arthritis in mice. *J. Immunol.* **2006**, *176* (10), 6254–6261. (g) Tsuji, F.; Oki, K.; Fujisawa, K.; Okahara, A.; Horiuchi, M.; Mita, S. Involvement of leukotriene B4 in arthritis models. *Life Sci.* **1999**, *64* (3), PL51–PL56. (h) Barnes, P. J. New treatments for COPD. *Nat. Rev. Drug Discovery* **2002**, *1* (6), 437–446. (i) Gompertz, S.; Stockley, R. A. A randomized, placebo-controlled trial of a leukotriene synthesis inhibitor in patients with COPD. *Chest* **2002**, *122* (1), 289–294. (j) Lemiere, C.; Pelissier, S.; Tremblay, C.; Chaboillez, S.; Thivierge, M.; Stankova, J.; Rola-Pleszczynski, R. Leukotrienes and isocyanate-induced asthma: a pilot study. *Clin. Exp. Allergy* **2004**, *34* (11), 1684–1689. (k) Luster, A. D.; Tager, A. M. T-cell trafficking in asthma: lipid mediators grease the way. *Nat. Rev. Immunol.* **2004**, *4* (9), 711–724. (l) Terawaki, K.; Yokomizo, T.; Nagase, T.; Toda, A.; Taniguchi, M.; Hashizume, K..; et al. Absence of leukotriene B4 receptor 1 confers resistance to airway hyperresponsiveness and Th2?type immune responses. *J. Immunol.* **2005**, *175* (7), 4217–4225. (m) Montuschi, P.; Sala, A.; Dahlen, S. E.; Folco, G. Pharmacological modulation of the leukotriene pathway in allergic airway disease. *Drug Discovery Today* **2007**, *12* (9−10), 404–412.

(8) (a) Brooks, D. W.; Summers, J. B.; Gunn, B. P.; Rodriques, K. E.; Martin, J. G.; Martin, M. B.; Mazdiyasni, H.; Holms, J. H.; Stewart, A. O.; Moore, J. L.; Young, P. R.; Albert, D. H.; Bouska, J. B.; Malo, P. E.; Dyer, R. D.; Bell, R. L.; Rubin, P.; Kesterson, J.; Carter, G. W. The discovery of A-64077, a clinical candidate for treating diseases involving leukotriene mediators. In *Abstracts of the International Chemical Congress of Pacific Basin Societies*; Honolulu, HI, 1989; BIOS 34 . (b) Sirois, P.; Borgeat, P.; Lauziere, M.; Dube, L.; Rubin, P. R.; Kesterson, J. Effect of zileuton (A-64077) on the 5-lipoxygenase activity of human whole blood ex vivo. *Agents Actions* **1991**, *34*, 117–120.

(9) Labelle, M.; Belley, M.; Gareau, Y.; Gauthier, J. Y.; Guay, D.; Gordon, R.; Grossman, S. G.; Jones, T. R.; Leblanc, Y.; McAuliffe, M.; McFarlane, C.; Masson, P.; Metters, K. M.; Ouimet, N.; Patrick, D. H.; Piechuta, H.; Rochette, C.; Sawyer, N.; Xiang, Y. B.; Pickett, C. B.; Ford-Hutchinson, A. W.; Zamboni, R. J.; Young, R. N. Discovery of MK-0476, a potent and orally active leukotriene D4 receptor antagonist devoid of peroxisomal enzyme induction. *Bioorg. Med. Chem. Lett.* **1995**, *5* (3), 283–288.

(10) Matassa, V. G.; Maduskuie, T. P.; Shapiro, H. S.; Hesp, B.; Snyder, D. W.; Aharony, D.; Krell, R. D.; Keith, R. A. Evolution of a Series of Peptidoleukotriene Antagonists: Synthesis and Structure/Activity Relationships of 1,3,5-Substituted Indoles and Indazoles. *J. Med. Chem.* **1990**, *33*, 1781–1790.

(11) Samuelsson, B.; Funk, C. D. Enzymes involved in the biosynthesis of leukotriene B4. *J. Biol. Chem.* **1989**, *264*, 19469–19472.

(12) (a) Lewis, R. A.; Austen, K. F.; Soberman, R. J. Leukotrienes and other products of the 5-lipoxygenase pathway. Biochemistry and relation to pathology in human diseases. *N. Engl. J. Med.* **1990**, *232*, 645–655. (b) Werz, O.; Steinhilber, D. Therapeutic options for 5-lipoxygenase inhibitors. *Pharmacol. Ther.* **2006**, *112*, 701–718.

(13) Mitsunobu, F.; Mifune, T.; Hosaki, Y.; Ashida, K.; Tsugeno, H.; Okamoto, M.; Takata, S.; Tanizaki, Y. Enhanced production of leukotrienes by peripheral leukocytes and specific IgE antibodies in patients with chronic obstructive pulmonary disease. *J. Allergy Clin. Immunol.* **2001**, *107*, 492–498.

(14) Okano-Mitani, H.; Ikai, K.; Imamura, S. Leukotriene A_4 hydrolase in peripheral leukocytes of patients with atopic dermatitis. *Arch. Dermatol. Res.* **1996**, *288*, 168–172.

(15) Klickstein, L. B.; Shapleigh, C.; Geotzl, E. J. Lipoxygenation of arachidonic acid as a source of polymorphonuclear leukocyte chemotactic factors in synovial fluid and tissue in rheumatoid arthritis and spondyloarthritis. *J. Clin. Invest.* **1980**, *66*, 1166–1170.

(16) (a) Penning, T. D.; Askonas, L. J.; Djuric, S. W.; Haack, R. A.; Yu, S. S.; Michener, M. L.; Krivi, G. G.; Pyla, E. Y. Kelatorphan and related analogs: Potent and selective inhibitors of leukotriene A4 hydrolase. *Bioorg. Med. Chem. Lett.* **1995**, *5*, 2517–2522. (b) Hogg, J. H.; Ollmann, I. R.; Haeggström, J. Z.; Wetterholm, A.; Samuelsson, B.; Wong, C. H. Amino hydroxamic acids as potent inhibitors of

leukotriene A4 hydrolase. *Bioorg. Med. Chem. Lett.* **1995**, *3*, 1405–1415. (c) Tsuji, F.; Miyake, Y.; Enomoto, H.; Horiuchi, M.; Mita, S. Effects of SA6541, a leukotriene A4 hydrolase inhibitor, and indomethacin on carrageenan-induced murine dermatitis. *Eur. J. Pharmacol.* **1998**, *346*, 81–85. (d) Grice, C. A.; Tays, K. L.; Savall, B. M.; Wei, J.; Butler, C. R.; Axe, F. U.; Bembenek, S. D.; Fourie, A. M.; Dunford, P. J.; Lundeen, K.; Coles, F.; Xue, X.; Riley, J. P.; Williams, K. N.; Karlsson, L.; Edwards, J. P. *J. Med. Chem.* **2008**, *51*, 4150–4169. (e) Rao, N. L.; Dunford, P. J.; Xue, X.; Jiang, X.; Lundeen, K. A.; Coles, F.; Riley, J. P.; Williams, K. N.; Grice, C. A.; Edwards, J. P.; Karlsson, L.; Fourie, A. M. *J. Pharmacol. Exp. Ther.* **2007**, *321*, 1154–1160. (f) Khim, S. K.; Bauman, J.; Evans, J.; Freeman, B.; King, B.; Kirkland, T.; Kochanny, M.; Lentz, D.; Liang, A.; Mendoza, L.; Phillips, G.; Tseng, J. L.; Wei, R. G.; Ye, H.; Yu, L.; Parkinson, J.; Guilford, W. J. *Bioorg. Med. Chem. Lett.* **2008**, *18*, 3895–3898. (g) Kirkland, T. A.; Adler, M.; Bauman, J. G.; Chen, M.; Haeggstrom, J. Z.; King, B.; Kochanny, M. J.; Liang, A. M.; Mendoza, L.; Phillips, G. B.; Thunnissen, M.; Trinh, L.; Whitlow, M.; Ye, B.; Ye, H.; Parkinson, J.; Guilford, W. J. *Bioorg. Med. Chem.* **2008**, *16*, 4963–4983. (h) Ye, B.; Bauman, J.; Chen, M.; Davey, D.; Khim, S. K.; King, B.; Kirkland, T.; Kochanny, M.; Liang, A.; Lentz, D.; May, K.; Mendoza, L.; Phillips, G.; Selchau, V.; Schlyer, S.; Tseng, J. L.; Wei, R. G.; Ye, H.; Parkinson, J.; Guilford, W. J. *Bioorg. Med. Chem. Lett.* **2008**, *18*, 3891–3894. (i) Enomoto, H.; Morikawa, Y.; Miyake, Y.; Tsuji, F.; Mizuchi, M.; Suhara, H.; Fujimura, K.; Horiuchi, M.; Ban, M. *Bioorg. Med. Chem. Lett.* **2009**, *19*, 442–446.

(17) Congreve, M.; Chessari, G.; Tisi, D.; Woodhead, A. J. Recent developments in fragment-based drug discovery. *J. Med. Chem.* **2008**, *51*, 3661–3689.

(18) Rees, D. C.; Congreve, M.; Murray, C. W.; Carr, R. Fragment-based lead discovery. *Nat. Rev. Drug Discovery* **2004**, *3*, 660–672.

(19) Congreve, M.; Carr, R.; Murray, C.; Jhoti, H. A "rule of three" for fragment-based lead discovery? *Drug Discovery. Today* **2003**, *8*, 876–877.

(20) Nienaber, V. L.; Greer, J. Discovering novel ligands for macromolecules using X-ray crystallographic screening. *Nat. Biotechnol.* **2000**, *18*, 1105–1108.

(21) Hopkins, A. L.; Colin, R.; Groom, C. R.; Alex, A. Ligand efficiency: a useful metric for lead selection. *Drug Discovery Today* **2004**, *9*, 430–431.

(22) Abad-Zapatero, C.; Metz, J. T. Ligand efficiency indices as guideposts for drug discovery. *Drug Discovery Today* **2005**, *10*, 464–469.

(23) Oprea, T.; Allu, T. R.; Fara, D. C.; Rad, R. F.; Ostopovici, L.; Bologa, C. G. Lead-like, drug-like or "Pub-like": how different are they? *J. Comput.-Aided Des.* **2007**, *21*, 113–119.

(24) Davies, D.; Mamat, B.; Magnusson, O.; Christensen, J.; Haraldsson, M.; Mishra, R.; Pease, B.; Hansen, E.; Singh, J.; Zembower, D.; Kim, H.; Kiselyov, A.; Burgin, A.; Gurney, M.; Stewart, L. Discovery of leukotriene A4 hydrolase inhibitors using metabolomics biased fragment crystallograph. *J. Med. Chem.* **2009**, *52*, 4694–4715.

(25) (a) Thunnissen, M. M.; Nordlund, P.; Haeggstrom, J. Z. Crystal structure of human leukotriene A(4) hydrolase, a bifunctional enzyme in inflammation. *Nat. Struct. Biol.* **2001**, *8*, 131–135. (b) Thunnissen, M. M.; Andersson, G. M.; Samuelsson, B.; Wong, B.; Haeggström, C. H.; Crystal, J. Z. Structures of leukotriene A4 hydrolase in complex with captopril and two competitive tight-binding inhibitors. *FASEB J.* **2002**, *16*, 1648–1650.

(26) Penning, T. D.; Chandrakumar, N. Z; Chen, B. B; Chen, H. Y.; Desai, B. N.; Djuric, S. W.; Docter, S. H.; Gasiecki, A. F.; Haack, R. A.; Miyashiro, J. M.; Russell, M. A. Structure−activity relationship studies on 1-[2-(4-phenylphenoxy)ethyl]pyrrolidine (SC-22716), a potent inhibitor of leukotriene A4 (LTA4) hydrolase. *J. Med. Chem.* **2002**, *43*, 721–735.

(27) A 1.9 Å resolution structure, 3FUD.pdb that contains a fragment bound on the surface of LTA_4H far from the active site (see ref 21), was used as reference for unligated active site topology.

(28) *Cerep*; http://www.cerep.fr/cerep/users/pages/catalog/Profiles/catalog.asp.

(29) Such a transformation has in fact been reported for SC-57461. Yuan, J. H.; Birkmeier, J.; Yang, D. C.; Hribar, J. D.; Liu, N.; Bible, R.; Hajdu, E.; Rock, M.; Schoenhard, G. Isolation and identification of metabolites of leukotriene A4 hydrolase inhibitor SC-57461 in rats. *Drug Metab. Dispos.* **1996**, *24*, 1124–1133.

(30) Yan, Z.; Caldwell, G. W. Metabolism profiling and cytochrome P450 inhibition and induction. *Drug Discovery Curr. Top. Med. Chem.* **2001**, *1*, 403–425.

(31) (a) Mitsunobu, O.; Yamada, M. *Bull. Chem. Soc. Jpn.* **1967**, *40*, 2380–2382. (b) Mitsunobu, O. *Synthesis* **1981**, 1–28.

(32) Wolfe, J. P.; Buchwald, S. L. Palladium-catalyzed amination of aryl iodides. *J. Org. Chem.* **1996**, *61*, 1133–1135.

(33) Gandolfi, C. A.; Di-Domenico, R.; Spinelli, S.; Gallico, L.; Fiocchi, L.; Lotto, A.; Menta, E.; Borghi, A.; Rosa, C. D.; Tognella, S. *N*-Acyl-2-substituted-1,3-thiazolidineas, new class of non-narcotic antitussive agents: Studies leading to the discovery of ethyl 2-[(2-methoxyphenoxy)methyl]-3-oxothiazolidine-3-propanoate. *J. Med. Chem.* **1995**, *38*, 508–525.

(34) Tagat, T.; Nishida, M. Palladium charcol-catlysed Suzuki−Miyaura coupling to obatin arylpyridines and arylquinolines. *J. Org. Chem.* **2003**, *68*, 9412–9415.

(35) Ma, D.; Qian, C. *N*,*N*-Dimethyl glycine-promoted Ullmann coupling reaction of phenols and aryl halides. *Org. Lett.* **2003**, *5* (21), 3799–3802.